The Meteoritical Society

Meteoritics & Planetary Science 43, Nr 9, 1531–1550 (2008)
Abstract available online at http://meteoritics.org

Refractory inclusions in the CH/CB-like carbonaceous chondrite Isheyevo: I. Mineralogy and petrography

Alexander N. KROT[1*], Alexander A. ULYANOV[2], and Marina A. IVANOVA[3]

[1]Hawai'i Institute of Geophysics and Planetology, School of Ocean and Earth Science and Technology, University of Hawai'i at Manoa, Honolulu, Hawai'i 96822, USA
[2]M. V. Lomonosov Moscow State University, Moscow 119992, Russia
[3]Vernadsky Institute of Geochemistry and Analytical Chemistry, Kosygin Street 19, Moscow 119991, Russia
*Corresponding author. E-mail: sasha@higp.hawaii.edu
Supplemental tables and figures are available at http://meteoritics.org/Online%20Supplements.htm

(Received 11 April 2007; revision accepted 08 April 2008)

Abstract–The CH/CB-like chondrite Isheyevo consists of metal-rich (70–90 vol% Fe,Ni-metal) and metal-poor (7–20 vol% Fe,Ni-metal) lithologies which differ in size and relative abundance of Fe,Ni-metal and chondrules, as well as proportions of porphyritic versus non-porphyritic chondrules. Here, we describe the mineralogy and petrography of Ca,Al-rich inclusions (CAIs) and amoeboid olivine aggregates (AOAs) in these lithologies. Based on mineralogy, refractory inclusions can be divided into hibonite-rich (39%), grossite-rich (16%), melilite-rich (19%), spinel-rich (14%), pyroxene-anorthite-rich (8%), fine-grained spinel-rich CAIs (1%), and AOAs (4%). There are no systematic differences in the inclusion types or their relative abundances between the lithologies. About 55% of the Isheyevo CAIs are very refractory (hibonite-rich and grossite-rich) objects, 20–240 μm in size, which appear to have crystallized from rapidly cooling melts. These inclusions are texturally and mineralogically similar to the majority of CAIs in CH and CB chondrites. They are distinctly different from CAIs in other carbonaceous chondrite groups dominated by the spinel-pyroxene ± melilite CAIs and AOAs. The remaining 45% of inclusions are less refractory objects (melilite-, spinel- and pyroxene-rich CAIs and AOAs), 40–300 μm in size, which are texturally and mineralogically similar to those in other chondrite groups. Both types of CAIs are found as relict objects inside porphyritic chondrules indicating recycling during chondrule formation.

We infer that there are at least two populations of CAIs in Isheyevo which appear to have experienced different thermal histories. All of the Isheyevo CAIs apparently formed at an early stage, prior to chondrule formation and prior to a hypothesized planetary impact that produced magnesian cryptocrystalline and skeletal chondrules and metal grains in CB, and possibly CH chondrites. However, some of the CAIs appear to have undergone melting during chondrule formation and possibly during a major impact event. We suggest that Isheyevo, as well as CH and CB chondrites, consist of variable proportions of materials produced by different processes in different settings: 1) by evaporation, condensation, and melting of dust in the protoplanetary disk (porphyritic chondrules and refractory inclusions), 2) by melting, evaporation and condensation in an impact generated plume (magnesian cryptocrystalline and skeletal chondrules and metal grains; some igneous CAIs could have been melted during this event), and 3) by aqueous alteration of pre-existing planetesimals (heavily hydrated lithic clasts). The Isheyevo lithologies formed by size sorting of similar components during accretion in the Isheyevo parent body; they do not represent fragments of CH and CB chondrites.

INTRODUCTION

The metal-rich CH and CB carbonaceous chondrites are among the most controversial groups of meteorites: both nebular and asteroidal models have been proposed to explain their anomalous chemistry, such as extreme enrichment in siderophile elements and extreme depletion in volatile elements, and unusual mineralogy (e.g., Grossman et al. 1988; Scott 1988; Weisberg et al. 1988; Wasson and Kallemeyn 1990; Bischoff et al. 1993; Meibom et al. 1999,

2000, 2001; Campbell et al. 2001, 2002; Krot et al. 2001a, 2002a, 2005a; Petaev et al. 2001a, 2001b; Rubin et al. 2003; Campbell and Humayun 2004).

The CH chondrites (Acfer 182, Allan Hills [ALH] 85085, Patuxen Range [PAT] 91546, Pecora Escarpment [PCA] 91467, Northwest Africa [NWA] 470, NWA 739, and NWA 770) contain high Fe,Ni-metal abundance (~20 vol%), dominant cryptocrystalline chondrules of small sizes (~20 μm), and rare, very refractory inclusions; the interchondrule, fine-grained matrix material is absent; heavily hydrated matrix-like lumps are common instead. Based on these unusual characteristics, Wasson and Kallemeyn (1990) concluded that the CH chondrites are modified "subchondritic" meteorites containing some chondrules and metal grains produced during a highly energetic asteroidal collision. More recently, based on the condensation origin of zoned Fe,Ni-metal grains (Meibom et al. 1999, 2000) and ^{16}O-enriched isotopic compositions of chondrules and refractory inclusions (Sahijpal et al. 1999; Kobayashi et al. 2003; Makide et al. 2004; Yoshitake et al. 2004), it has been argued that refractory inclusions, chondrules, and zoned metal grains in CH chondrites are in fact pristine nebular products (Krot et al. 2002a).

The CB chondrites (Bencubbin, Gujba, Weatherford, Hammadah al Hamra [HaH] 237, Queen Alexandra Range [QUE] 94411 paired with QUE 94627, and MacAlpine Hills [MAC] 02675) contain much higher abundance of metal (~70 vol%) and bigger chondrules (100 μm–7 mm) than CH chondrites. In contrast to CH chondrites, the CB chondrules have exclusively non-porphyritic (cryptocrystalline and skeletal) textures. Largely based on sizes of the chondritic components, the CB meteorites are currently divided into two subgroups (CB_a [Bencubbin, Gujba, Weatherford] and CB_b [HaH 237, QUE 94411, QUE 94627, and MAC 02675] [Weisberg et al. 2001]), which, however, may represent two lithologies from the same parent asteroid (Krot et al. 2005a). Similar to CH chondrites, the CB_b meteorites contain chemically zoned metal condensates, which, however, are much more abundant than in CH chondrites (Meibom et al. 2001; Petaev et al. 2001a; Weisberg et al. 2001), and rare refractory inclusions (Krot et al. 2001b). Based on the young chondrule ages (4562.7 ± 0.5 Myr), lack of evidence for recycling of chondrules and zoned metal grains, and lack of interchondrule, fine-grained matrix material, Krot et al. (2005a) concluded that CB chondrites formed from a vapor-melt plume produced by a giant impact between planetary embryos after dust in the protoplanetary disk had largely dissipated. The origin of CAIs in CB chondrites remains poorly understood. In contrast to the majority of CAIs in different chondrite groups, those from HaH 237 and QUE 94411 are ^{16}O-poor (Krot et al. 2001a) and show no excess of ^{26}Mg (Gounelle et al. 2006), consistent with either late-stage formation, after decay of ^{26}Al, or with late-stage re-equilibration with a gaseous reservoir having isotopically normal magnesium and oxygen isotopic composition (e.g., impact-generated plume). Alternatively, the CB CAIs might have formed early in the nebular region lacking ^{26}Al.

Although it has been previously noticed that non-porphyritic chondrules, zoned metal grains, metal-sulfide grains, and refractory inclusions in CH chondrites are mineralogically similar to those in CB chondrites (e.g., Krot et al. 2001b, 2002a; Meibom et al. 2001; Weisberg et al. 2001; Campbell and Humayun 2004), a genetic relationship between these metal-rich meteorites (if any) is yet to be understood. The recently discovered metal-rich chondrite Isheyevo (Ivanova et al. 2008) contains the metal-rich (70–90 vol% Fe,Ni-metal) and the metal-poor (7–20 vol% Fe,Ni-metal) lithologies which show some mineralogical similarities to both CH and CB_b chondrites. They contain abundant zoned Fe,Ni-metal grains (like CB_b chondrites), porphyritic and non-porphyritic chondrules (like CH chondrites), heavily hydrated matrix lumps (like CH and CB chondrites), and rare (<1 vol%) refractory inclusions; no fine-grained, matrix-like material is observed around these coarse components (like CH and CB chondrites). Isheyevo may have experienced mild thermal metamorphism (some zoned Fe,Ni-metal grains are decomposed), but appears to have largely escaped post-accretion aqueous alteration (Krot et al. 2008a). Since this meteorite can potentially provide a clue for a genetic relationship between the CH and CB chondrites and for the origin of metal-rich chondrites in general, we initiated detailed mineralogical and isotopic studies of its components.

Krot et al. (2008a) described the mineralogy and petrography of chondrules in Isheyevo. They concluded that there are two generations of chondrules: one is mineralogically similar to chondrules in CB chondrites and another is mineralogically similar to porphyritic chondrules in CH chondrites. Based on these observations, Krot et al. (2008a) suggested that some of the chondrules and metal grains in Isheyevo, and possibly in CH chondrites, formed in an impact generated plume. Here we report mineralogy and petrography of CAIs and AOAs in Isheyevo and compare them with the previously studied refractory inclusions in the CB_b (Krot et al. 2001b) and CH chondrites (MacPherson et al. 1989; Kimura et al. 1993; Weber and Bischoff 1994; Weber et al. 1995a, 1995b; Krot et al. 1999a, 1999b, 2006a; Ivanova et al. 2001, 2002). The preliminary results of this study have been reported by Krot et al. (2006b).

ANALYTICAL PROCEDURES

Fourteen polished sections of Isheyevo (*MAI-1*, *AAU-l*, *AAU-s*, *UH-p*, *UH-5g*, *UH 9–1*, *–2*, *–3*, *–4*, *–5*, *–6*, *–7*, *–8*, *–9*) of ~30 cm^2 were mapped in Ca, Al, Mg, Ti, Na, Si, Ni, and Co Kα X-rays using fully focused electron beam, 15 kV accelerating voltage, 100 nA beam current, 20–30 ms per pixel acquisition time, and resolution of ~8–10 μm per pixel with a Cameca SX-50 electron microprobe at University of Hawai'i and a Cameca SX-100 at Vernadsky Institute. The elemental maps in Mg, Ca, and Al K were combined using an

RGB-color scheme (Mg - red, Ca - green, Al - blue) and ENVI (environment for visualizing images) software package. The identified refractory inclusions were studied in the backscattered electron (BSE) mode with the JEOL 5900 LV scanning electron microscope (SEM) equipped with an energy dispersive spectrometer (EDS). Mineral compositions were determined with the Cameca SX-50 and SX-100 electron microprobes using 15 kV accelerating voltage and beam currents of 10–20 nA. Counting times on both peak and background were 10 s for Na and K and 30 s for all other elements. Minerals were analyzed with a focused (1–2 μm) beam. Well-characterized silicates and oxides were used as standards. Matrix corrections were applied using a PAP software routine. Detection limits in silicates were (in wt%) SiO_2, Al_2O_3, MgO, TiO_2, CaO, K_2O–0.04; Na_2O, Cr_2O_3–0.06; MnO–0.07; FeO–0.08.

RESULTS

Metal-Rich and Metal-Poor Lithologies and Abundance of Refractory Inclusions

X-ray mapping of Isheyevo revealed the presence of the metal-rich (~70–90 vol% Fe,Ni-metal) and the metal-poor (~7–20 vol% Fe,Ni-metal) lithologies (Ivanova et al. 2008). There is typically a gradual transition between the lithologies; no clasts composed of different lithologies have been observed. The lithologies consist of Fe,Ni-metal, chondrules, refractory inclusions, and heavily hydrated matrix lumps; they differ in size and relative abundance of Fe,Ni-metal and chondrules as well as proportions of porphyritic versus non-porphyritic chondrules (Fig. A1) (all supplemental material is available at http://meteoritics.org/Online%20Supplements.htm). Since porphyritic chondrules are generally larger than non-porphyritic, the differences in abundance of chondrules with different textures among the lithologies could be a result of differences in sizes.

The metal-rich lithologies are texturally and mineralogically most similar to the CB_b chondrites Hammadah al Hamra 237, QUE 94411, QUE 94627, and MAC 02675. They are dominated by chemically zoned Fe,Ni-metal grains and non-porphyritic (cryptocrystalline and skeletal) chondrules. However, the common presence of porphyritic chondrules in the metal-rich lithologies does not allow these lithologies to be classified as CB_b chondritic materials.

The metal-poor lithologies are similar in metal abundance and chondrule textures (both porphyritic and non-porphytic textures are common) to CH chondrites (Krot et al. 2002a). In contrast to CH chondrites, however, ~20% of metal grains in these lithologies are chemically zoned (Fig. EA1b).

Because the most metal-rich and the most metal-poor lithologies are volumetrically minor in the sections studied and contain only rare CAIs (Ivanova et al. 2006), all refractory inclusions described below are from lithologies with 70 vol% and 20 vol% of Fe,Ni-metal. The abundance of CAIs in both lithologies is ~1 vol%.

Calcium-Aluminum-Rich Inclusions and Amoeboid Olivine Aggregates

Based on mineralogy, ~330 refractory inclusions identified in Isheyevo can be divided into pyroxene ± hibonite ± melilite ± spinel and hibonite-melilite-rich (37%), grossite-rich/-bearing (18%), melilite-rich (23%), spinel-rich, including isolated spinel grains (16%), pyroxene-anorthite-rich (5%) CAIs, and amoeboid olivine aggregates (AOAs) (1%). There are no systematic differences in the relative proportions of CAIs of different mineralogical types and AOAs between the lithologies. To illustrate this observation, CAIs of different types and AOAs from both the metal-rich and metal-poor lithologies are included in Figs. 1–11.

Pyroxene ± hibonite ± melilite ± spinel inclusions have compact, igneous textures and consist of Al-diopside (solid solution of $CaMgSi_2O_6$ – $CaAl_2SiO_6$ – $CaAlTiSiO_6$), melilite, hibonite, and spinel; perovskite is minor or accessory (Fig. 1). There are significant variations in grain sizes and modal mineralogy of the CAIs, with pyroxene and melilite being the dominant phases (Figs. 1a and 1b). Spinel, if present, forms coarse euhedral crystals, often containing inclusions of hibonite (Fig. 1c); sizes of the hibonite inclusions are similar to those in the pyroxene-melilite groundmass of the host CAIs (Fig. 1b). Some of the CAIs consist either entirely of Al-diopside or of Al-diopside with inclusions of forsteritic olivine (Fig. 1d). The forsterite-bearing CAIs are commonly surrounded by monomineralic rims of forsterite (Fig. 1d); rims around more refractory CAIs are generally absent (Figs. 1a and 1b). The melilite-bearing CAIs contain no or very little secondary anorthite (Fig. 1c).

Melilite in the pyroxene-hibonite-melilite-spinel CAIs is highly gehlenitic (Table A1). Pyroxenes are Ti-poor and show significant variations in Mg and Al contents within an individual spherule (Table A2; Fig. A2). Hibonite is Mg- and Ti-poor (Table A3; Fig. A3). Spinel is poor in Cr and Fe (Table A4). Forsterite has high Ca contents (Table A5).

Hibonite-melilite-rich CAIs are mineralogically similar to the pyroxene ± hibonite ± melilite ± spinel CAIs described above, but generally lack Al-diopside. These are spheroidal or ellipsoidal objects composed of hibonite, melilite, perovskite, grossite, and spinel (Fig. 2). There are significant variations in modal mineralogy of the hibonite-melilite-rich CAIs with melilite (Figs. 2a–c), hibonite (Figs. 2d and 2e), and, occasionally, grossite (Fig. 2f) being the dominant phases. Hibonite typically forms euhedral crystals embedded in melilite. In the very hibonite-rich CAIs, melilite occupies interstitial regions between the hibonite grains. Perovskite is a minor phase, except one of the CAIs where it is concentrated in a core (Fig. 2a). Most of the hibonite-rich CAIs, if not fragmented, are surrounded by a continuous layer

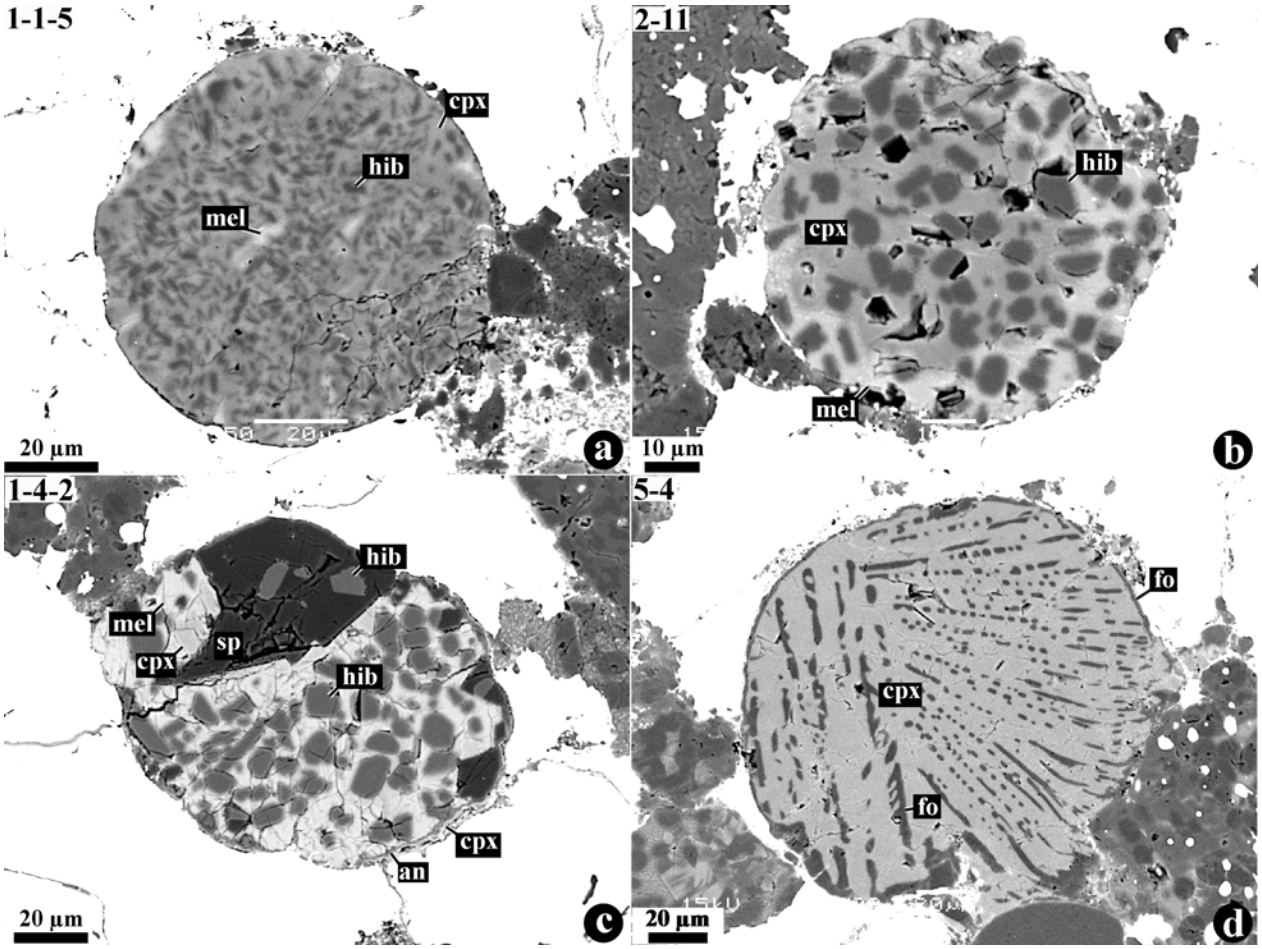

Fig. 1. BSE images of the pyroxene-hibonite-melilite-spinel CAIs (a–c) and a pyroxene-forsterite CAI (d). CAI *1-4-2* is surrounded by a thin double-layered rim of anorthite and Al-diopside. CAI *5-4* is surrounded by a thin forsterite rim. Abbreviations: an = anorthite; cpx = Al-diopside; fo = forsterite; hib = hibonite; mel = melilite; sp = spinel. The same abbreviations (unless stated) are used in other figure captions as well. a, c) Metal-rich lithology; b, d) metal-poor lithology.

of melilite and a thin rim of Al-diopside (Fig. 2a); the melilite shows no or little evidence for replacement by anorthite (Fig. 2b). One of the hibonite-rich CAIs is rimmed by a thick, igneous rim of Al-diopside and forsterite (Fig. 2c). Spinel, if present, is typically concentrated in outer portions of the CAIs (Fig. 2c). Occasionally, spinel together with melilite forms thick mantles around hibonite-melilite cores; spinel in these mantles has prismatic morphology and may pseudomorph hibonite (Fig. 2d).

Some hibonite-rich CAIs are surrounded by a thick mantle of grossite with perovskite inclusions and melilite (Figs. 2e and 2f). One of these CAIs is surrounded by a double-layered rim of spinel + hibonite and melilite (Fig. 2f).

Melilite in the hibonite-rich CAIs is highly gehlenitic (Table A1). Hibonite is Mg- and Ti-poor (Table A3). Spinel is poor in Cr and Fe (Table A4).

Grossite-rich CAIs are compact, ellipsoidal or irregularly shaped objects composed largely of grossite, melilite, Al-diopside, and spinel; perovskite and hibonite are generally minor or accessory. There are significant textural variations among grossite-rich CAIs (Figs. 3 and 4). Some of the grossite-rich CAIs appear to be unmelted (Fig. 3). In these CAIs, grossite, perovskite, or osbornite (TiN-TiC solid solution, Meibom et al. 2007) form cores, whereas melilite forms mantles and rims (outside spinel layer) around the inclusions (Figs. 3a–d). In spite of the presence of melilite in the outermost parts of the grossite-rich CAIs, anorthite replacing melilite is either absent or very minor; melilite is often surrounded by a thin layer of Al-diopside (Figs. 3a and 3b). In some of the CAIs, grossite appears to be corroded by melilite (Figs. 3c–e). Similar corrosion relationships between grossite and melilite were described in the grossite-rich CAIs from the CH carbonaceous chondrite NWA 739 and attributed to gas-solid reactions (Krot et al. 2006a). In most cases, however, grossite forms rounded-to-subhedral inclusions in melilite (Fig. 4a) or Al-diopside (Figs. 4b–d), intergrowths with melilite (Fig. 4e), or occupies interstitial regions between grossite grains suggesting an igneous origin (Fig. 4f). The igneous origin is consistent with the presence of coarse euhedral spinel grains and platy hibonites intergrown with grossite and melilite (Figs. 4a–d).

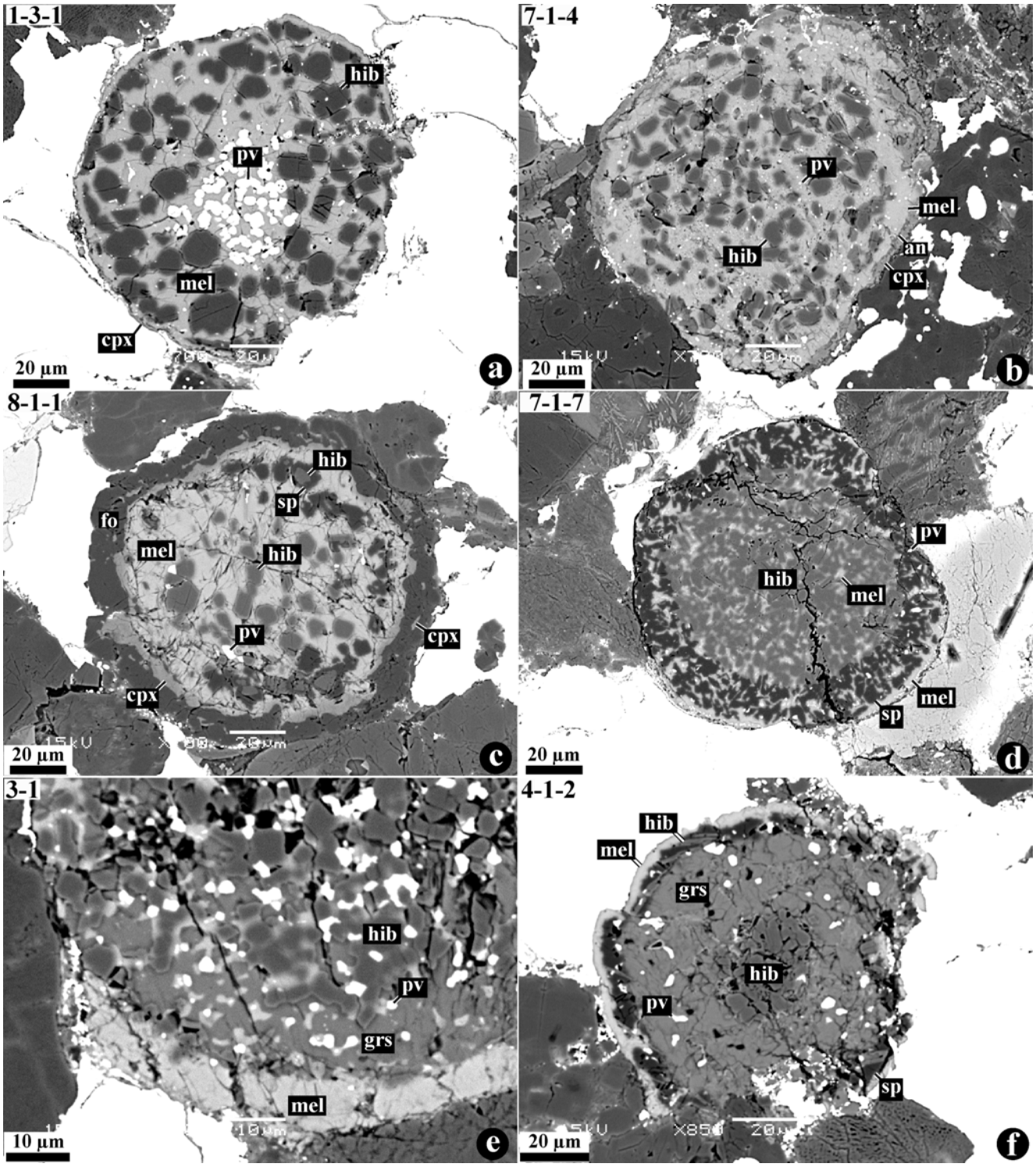

Fig. 2. BSE images of the hibonite-melilite-rich CAIs. a) Melilite-hibonite CAI with a perovskite-rich core and a thin melilite-diopside rim. b) Melilite-hibonite CAI rimmed by pyroxene; melilite is slightly replaced by anorthite. c) Melilite-hibonite-spinel CAI surrounded by a thick igneous layer of Al-diopside and forsterite. d) Hibonite-melilite core surrounded by a thick mantle of spinel and melilite, and a thin melilite rim. e) Hibonite-melilite-perovskite core surrounded by a grossite-melilite-perovskite mantle and a rim of melilite. f) Hibonite-perovskite core surrounded by a thick mantle of grossite and a double-layered rim of spinel + hibonite + perovskite and melilite. grs = grossite. a–d) metal-poor lithology; e, f) Metal-rich lithology.

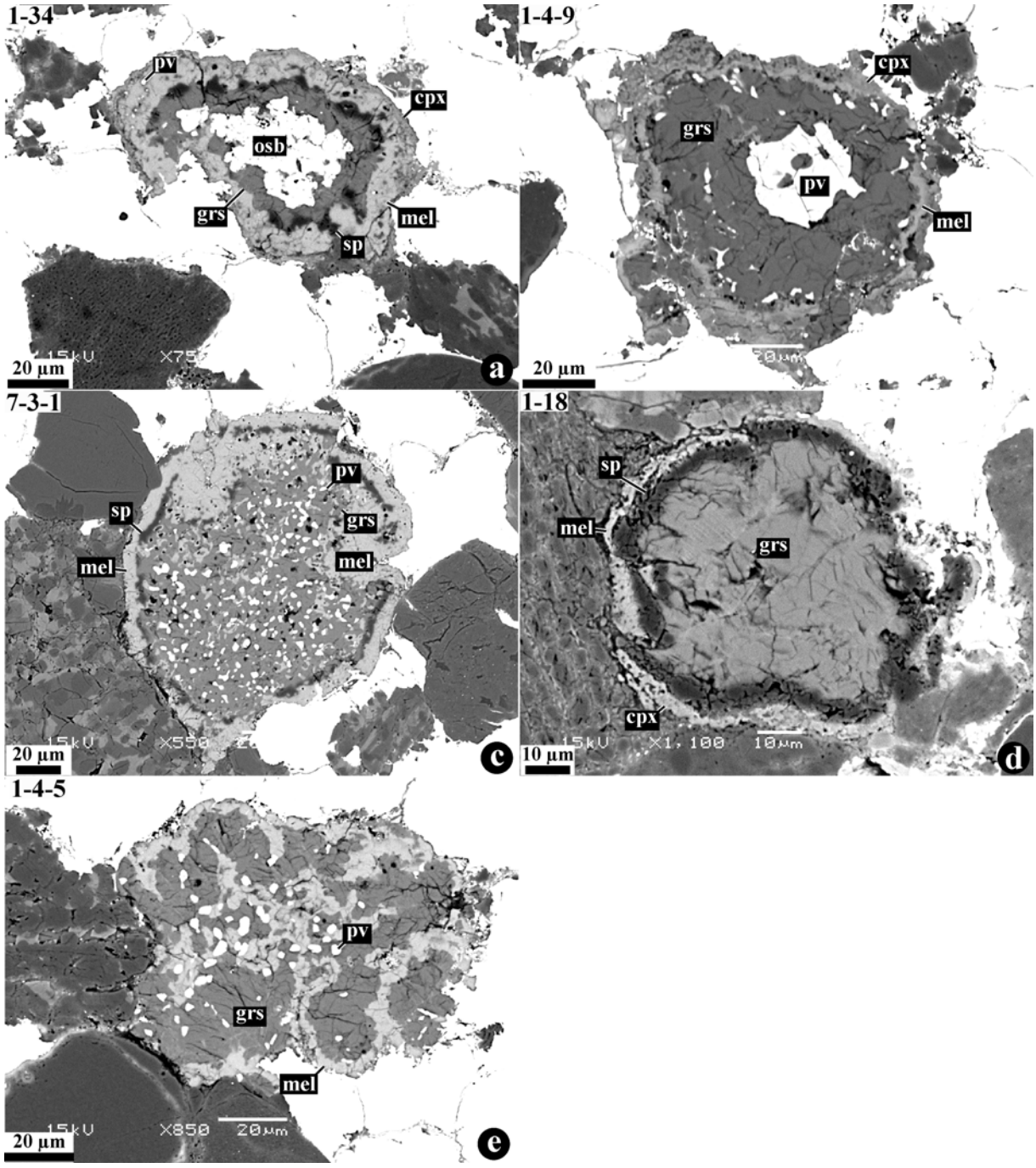

Fig. 3. BSE images of the grossite-rich CAIs. a) Concentrically zoned CAI having a polycrystalline osbornite (osb) core, grossite mantle, and rims of spinel, melilite, and Al-diopside. b) Grossite CAI with a perovskite core. The CAI is rimmed by melilite and Al-diopside. c) Grossite-perovskite-melilite core rimmed by spinel and melilite. d) Grossite CAI rimmed by spinel, melilite, and Al-diopside. e) Multiple, irregularly shaped grossite-perovskite cores rimmed by melilite; melilite appears to replace grossite. a, b, c) Metal-rich lithology; d, e) metal-poor lithology.

Some of the grossite-rich CAIs are mineralogically zoned (Figs. 4c, 4d, and 4f). CAI C2 has a grossite-melilite core surrounded by a thick, melilite-free grossite mantle and by a thin melilite rim; numerous perovskite inclusions occur in both the core and the mantle (Fig. 4f). A pyroxene-grossite-hibonite core of the CAI *6–1* is surrounded by a melilite mantle of variable thickness and mineralogy (Figs. 4c and 4d). The melilite mantle on one side of the CAI is relatively thin and contains abundant inclusions of perovskite and Al-Ti-rich pyroxene (Fig. 4d), whereas on the opposite side, the mantle is thick and free of perovskite and pyroxene inclusions.

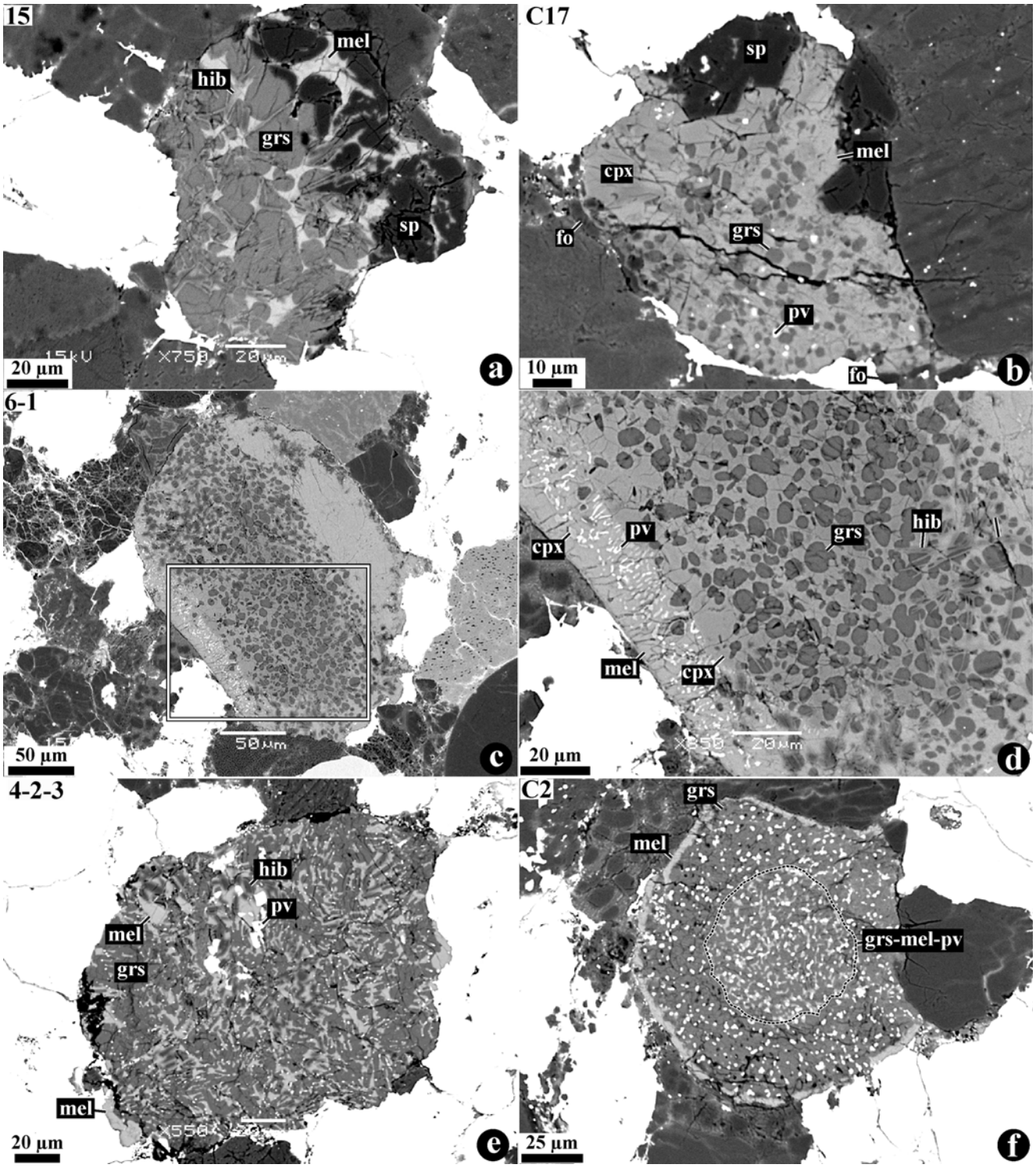

Fig. 4. BSE images of the igneous, grossite-rich CAIs. a) Coarse-grained grossite-melilite-spinel-hibonite CAI; platy hibonites form inclusions in grossite, spinel, and melilite and crosscut intergrain boundaries. b) Coarse-grained, grossite-bearing, melilite-pyroxene-spinel CAI fragment rimmed by forsterite; perovskite is minor. c, d) Pyroxene-grossite-hibonite core surrounded by a melilite mantle of variable thickness and mineralogy: on the left (see "d"), it is thin and contains abundant inclusions of perovskite and Al-Ti-diopside; on the right, it is thick and perovskite-free. e) Grossite-melilite-hibonite-perovskite CAI. Hibonite and coarse perovskite grains are concentrated in the melilite-rich region. f) Concentrically zoned grossite-melilite-perovskite CAI. Melilite is concentrated in the core (outlined) filling interstitial regions between grossite grains; it also forms a monomineralic layer around the inclusion. The grossite-perovskite mantle is melilite-free. a, c, d) Metal-poor lithology; b, e, f) metal-rich lithology.

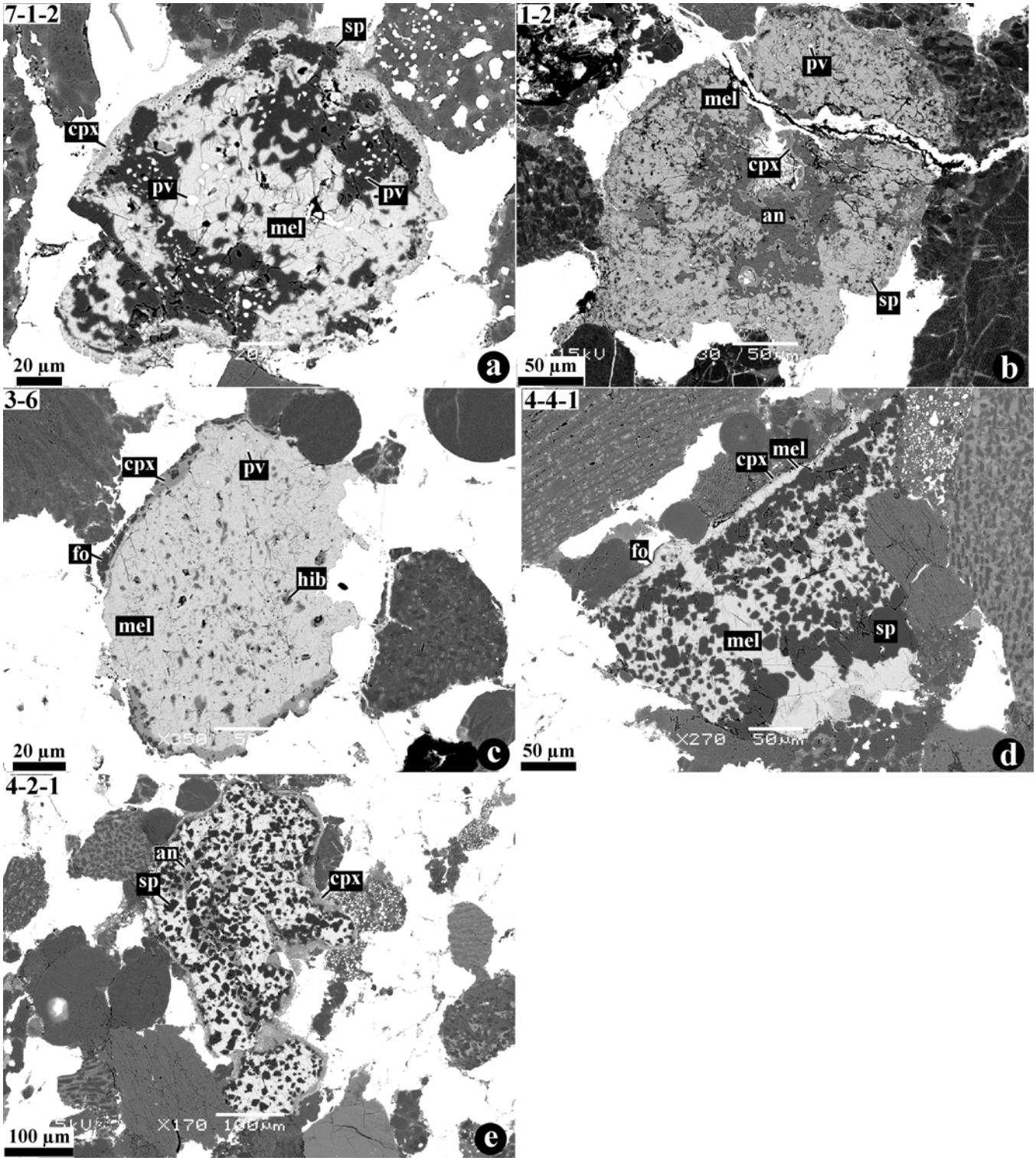

Fig. 5. BSE images of the melilite-rich (type A) CAIs. a) Melilite-spinel CAI with anhedral spinel grains forming irregularly shaped regions in melilite; perovskite is minor. The CAI is surrounded by a rim of Al-diopside. b) Irregularly shaped melilite CAI rimmed by Al-diopside; spinel is accessory; perovskite is minor. Melilite is extensively replaced by anorthite. c) Compact (igneous?) melilite CAI with small subhedral inclusions of hibonite; perovskite is minor. The CAI is surrounded by a compact Al-diopside-forsterite rim. d) An igneous melilite-spinel CAI surrounded by a double-layered rim of Al-diopside and forsterite. f) Melilite-spinel CAI extensively replaced by anorthite and rimmed by Al-diopside. a) Metal-poor lithology; b–e) metal-rich lithology.

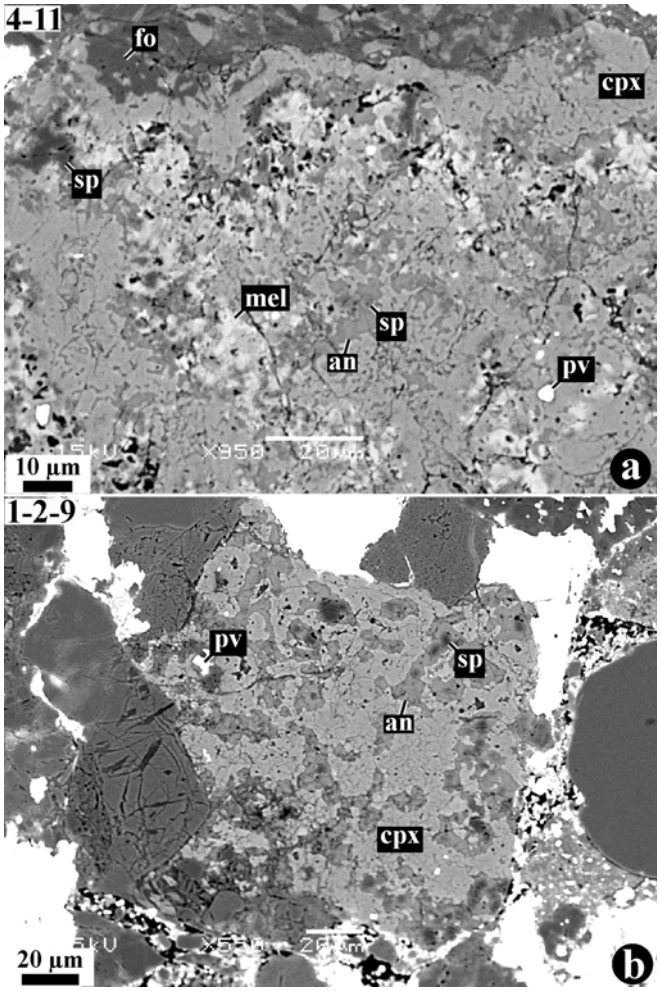

Fig. 6. BSE images of the irregularly shaped pyroxene-melilite-spinel-anorthite CAIs with melilite and spinel replaced to various degrees by anorthite and Al-diopside; perovskite is minor. CAI *4–11* is surrounded by the Al-diopside and forsterite rims. a, b) Metal-poor lithology.

Grossite and perovskite of the grossite-rich CAIs are nearly pure $CaAl_4O_7$ and $CaTiO_3$, respectively (Table A5). Osbornite contains some carbon and must be a TiN-TiC solid solution (Meibom et al. 2007). Melilite is highly gehlenitic (Table A1). Spinel is poor in Cr and Fe (Table A4).

Melilite-rich CAIs are either irregularly shaped (Figs. 5a and 5b) or ellipsoidal (Fig. 5c) objects composed largely of melilite, spinel, and minor or accessory Al-Ti-diopside, hibonite, and perovskite. Some of the melilite-rich CAIs contain anhedral spinel grains (Fig. 5a); others contain euhedral or subhedral hibonite (Fig. 5c) or spinel grains (Figs. 5d and 5e). Melilite is replaced by anorthite to various degrees (Figs. 5b and 5e). The melilite-rich CAIs are surrounded by Al-diopside rims (Figs. 5a and 5e) or by Al-diopside + forsterite rims (Figs. 5c and 5d).

Melilite of the melilite-rich CAIs is slightly more åkermanitic than those of the hibonite-rich and grossite-rich CAIs (Table A1; Fig. A4). Pyroxenes contain high Ti and Al contents (Table A2; Fig. A2). Anorthite is compositionally pure $CaAl_2Si_2O_8$ (Table A6). Spinel is poor in Cr and Fe (Table A4). Olivine is nearly pure forsterite (Table A5).

Pyroxene-anorthite-rich CAIs consist mainly of Al-diopside, anorthite, spinel, and ± melilite; perovskite is minor or absent (Figs. 6 and 7). Based on the textures, these CAIs can be divided into non-igneous (Fig. 6) and igneous (Fig. 7). The apparently non-igneous CAIs contain abundant secondary anorthite replacing melilite and spinel and are surrounded by the Al-diopside ± forsterite rims. The igneous anorthite-rich (type C) CAIs consist of lath-shaped anorthite, euhedral or subhedral spinel, Al-diopside, and melilite (Figs. 7a and 7b). Aluminum-diopside occurs as igneous mantles around CAIs (Fig. 7a) or in interstitial regions between anorthite laths, together with minor melilite (Fig. 7b).

Several type C CAIs contain Fe,Ni-metal and subhedral grains of olivine and low-Ca pyroxene overgrown by Al-diopside; melilite, spinel, hibonite, and perovskite are accessory (Figs. 7c–f). None of these CAIs have Wark-Lovering rims. These observations and the fact that ferromagnesian olivine and low-Ca pyroxene are the major chondrule minerals, which are generally absent in igneous CAIs, suggest that the olivine- and low-Ca-pyroxene-bearing type C CAIs are hybrid objects; i.e., they were probably melted together with ferromagnesian chondrule precursors during chondrule-forming events (Krot et al. 2005b).

Fine-grained spinel-rich CAIs consist of multiple concentrically zoned objects having a spinel + perovskite core rimmed by melilite and Al-diopside (Fig. 8a). In some CAIs, melilite is nearly completely replaced by anorthite (Figs. 8b and 8c).

Spinel-rich CAIs consist of spinel, melilite, and Al-diopside; perovskite is minor or absent (Fig. 9). There is a continuum between these CAIs and the melilite-rich and pyroxene-rich CAIs. Based on the textures, the spinel-rich CAIs can be divided into 1) irregularly shaped or ellipsoidal objects composed of anhedral spinel grains and surrounded by melilite and Al-diopside (Fig. 9a), and 2) rounded or ellipsoidal igneous inclusions with coarse, euhedral spinel and ± forsterite grains embedded in Al-diopside of variable chemical composition, and minor melilite (melilite is often absent); the latter are commonly rimmed by forsterite (Figs. 9b–d). Melilite of the irregularly shaped CAIs is often replaced by anorthite; no anorthite was found in the coarse-grained, igneous CAIs. The Al-diopside in the apparently igneous CAIs shows large variations in Al contents, clearly visible as variations in brightness in BSE images (Figs. 9c and 9d).

Amoeboid olivine aggregates (AOAs) consist of forsteritic olivine, often enclosing Fe,Ni-metal, and a refractory component composed of Al-diopside, anorthite, minor spinel, and rarely melilite (Fig. 10). There are large variations in modal abundances of forsterite and Ca-Al-rich

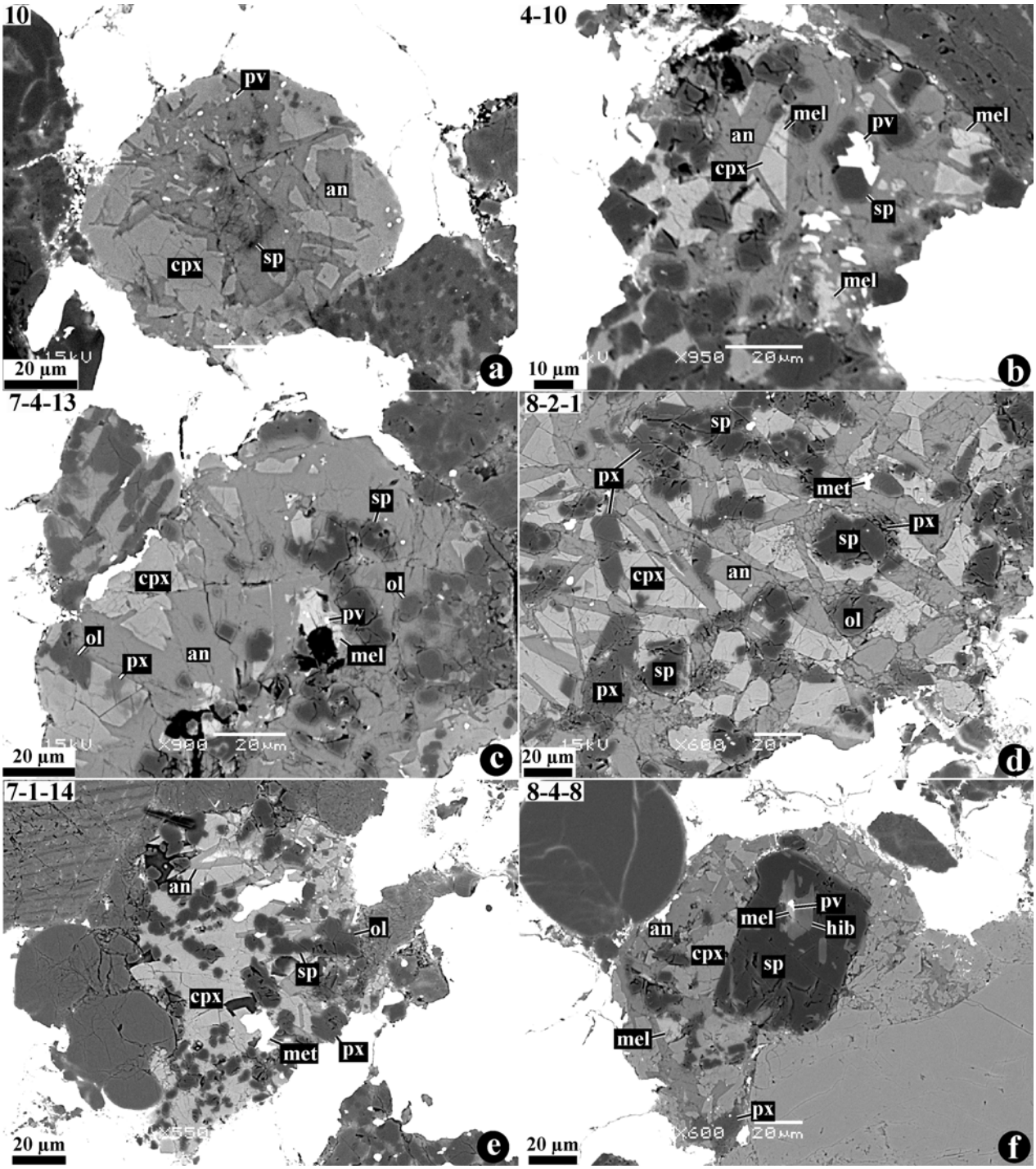

Fig. 7. BSE images of the igneous, pyroxene-anorthite ± melilite (type C) CAIs composed of lath-shaped anorthite, Al,Ti-diopside, subhedral-to-euhedral spinel, ± interstitial melilite, and perovskite. Type C CAIs shown in "c–f" are associated with ferromagnesian olivine and low-Ca pyroxene. c) CAI consists of lath-shaped anorthite, subhedral-to-euhedral spinel and olivine grains, and interstitial Al-rich clinopyroxene (cpx) with inclusions of low-Ca pyroxene (px), and melilite with inclusions of perovskite. d) CAI consists of lath-shaped anorthite, subhedral grains of spinel overgrown by Al-bearing low-Ca pyroxene, olivine, and interstitial high-Ca pyroxene; Fe,Ni-metal is minor. e) CAI is composed of Al-diopside, lath-shaped anorthite, spinel, forsteritic olivine, and Fe,Ni-metal. f) CAI contains large spinel grain with a polymineralic inclusion of hibonite, melilite, and perovskite. It is surrounded by an igneous material of lath-shaped anorthite, Al-diopside, spinel, and minor melilite and low-Ca pyroxene. None of the type C CAIs have Wark-Lovering rims around them. a, b, d–f) Metal-poor lithology; c) metal-rich lithology.

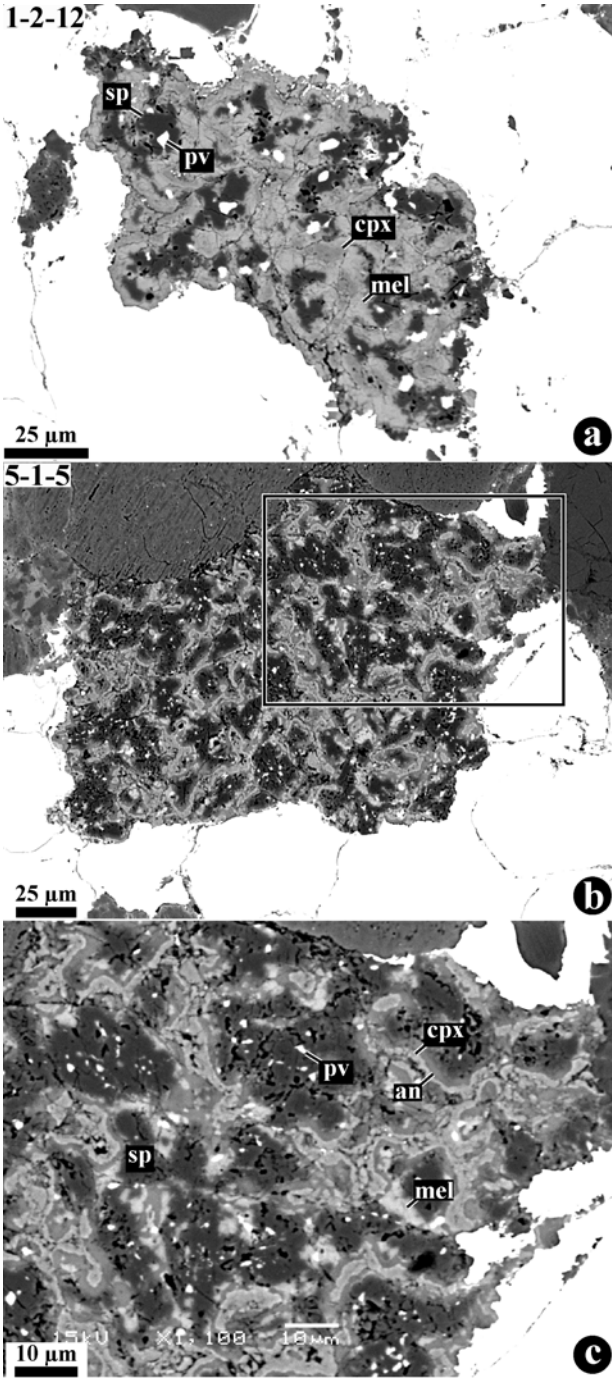

Fig. 8. BSE images of the fine-grained, spinel-rich CAIs composed of concentrically zoned objects having a spinel + perovskite core surrounded by the layers of melilite and Al-diopside. In CAI *5-1-15* melilite is almost entirely replaced by anorthite. a–c) Metal-rich lithology.

minerals (Figs. 10a–c). Like in AOAs from other carbonaceous chondrites (Krot et al. 2004a, 2004b), forsterite in outer portions of some of the Isheyevo AOAs is replaced by low-Ca pyroxene (Fig. 10a). The refractory component is often mineralogically zoned, with spinel grains surrounded by the layers of anorthite and Al-diopside. Occasionally, Al-diopside and forsterite occur as subhedral grains surrounded by anorthite, possibly indicating melting (Fig. 10c).

One of the melilite-rich CAIs is surrounded by a thick, layer of Al-diopside and a thick forsterite-rich rim (Fig. 10d). Melilite is replaced by a fine-grained mixture of Al-diopside and spinel. This object can be considered as AOA that is dominated by a refractory component (Krot et al. 2004a) or as the melilite-rich CAI surrounded by the forsterite-rich accretionary rim (Krot et al. 2001c).

Relict Calcium-Aluminum-Rich Inclusions Inside Chondrules

Like in many chondrite groups, some of the CAIs either occur inside chondrules (Figs. 11a–d) or are surrounded by chondrule-like igneous rims (Fig. 11e) (e.g., Russell et al. 2005). In both cases, these CAIs were mixed with ferromagnesian silicate precursors and melted during chondrule-forming events, i.e., they can be classified as relict objects inside chondrule melts.

The most common type of relict CAIs inside the Isheyevo chondrules are spinel-rich. They consist of spinel, anorthite, and minor perovskite (Figs. 11a–c). Anorthite occupies interstitial regions between spinel grains and forms monomineralic layers around spinel cores. The anorthite may have replaced melilite commonly associated with the spinel-rich CAIs (Fig. 9a). Chondrule *1-3-3* contains a large spinel grain corroded by the chondrule melt (Fig. 11c). Such coarse spinel grains are characteristic for the igneous, spinel-rich CAIs in Isheyevo (e.g., Figs. 9b and 9c). Chondrule *1-3-5* contains relict hibonite CAI surrounded by a spinel layer, which is corroded by the plagioclase-normative glass of the host chondrule (Fig. 11d). The host chondrules containing relict CAIs have exclusively porphyritic textures and consist of forsteritic olivine, low-Ca pyroxene, high-Ca pyroxene, anorthitic plagioclase, ±silica, and Fe,Ni-metal nodules.

The grossite-rich CAI *43* (Fig. 11e) is rimmed by spinel, plagioclase-normative glassy (?) material, and an igneous layer of forsteritic olivine, low-Ca pyroxene, and high-Ca pyroxene. All minerals in the igneous layer contain tiny nodules of Fe,Ni-metal.

In addition to the CAI-bearing chondrules, some of the chondrules consist of the mineralogically distinct portions—Al–rich and ferromagnesian (Fig. A6). The ferromagnesian portions consist of forsteritic olivine, low-Ca pyroxene, high-Ca pyroxene, glassy or microcrystalline mesostasis, and Fe,Ni-metal; the Al-rich portions are metal-free and dominated by high-Ca pyroxene, anorthitic plagioclase, and ±spinel. Most of these chondrules are Al-rich, i.e., contain >10 wt% Al_2O_3 (Bischoff and Keil 1984). Similar chondrules have been previously described in the CR, CV, and ungrouped carbonaceous chondrites Acfer 094 and Adelaide and attributed to incomplete homogenization of the CAI-like and ferromagnesian chondrule melts during chondrule formation (e.g., Krot et al. 2001d, 2002b, 2004c; Krot and Keil 2002).

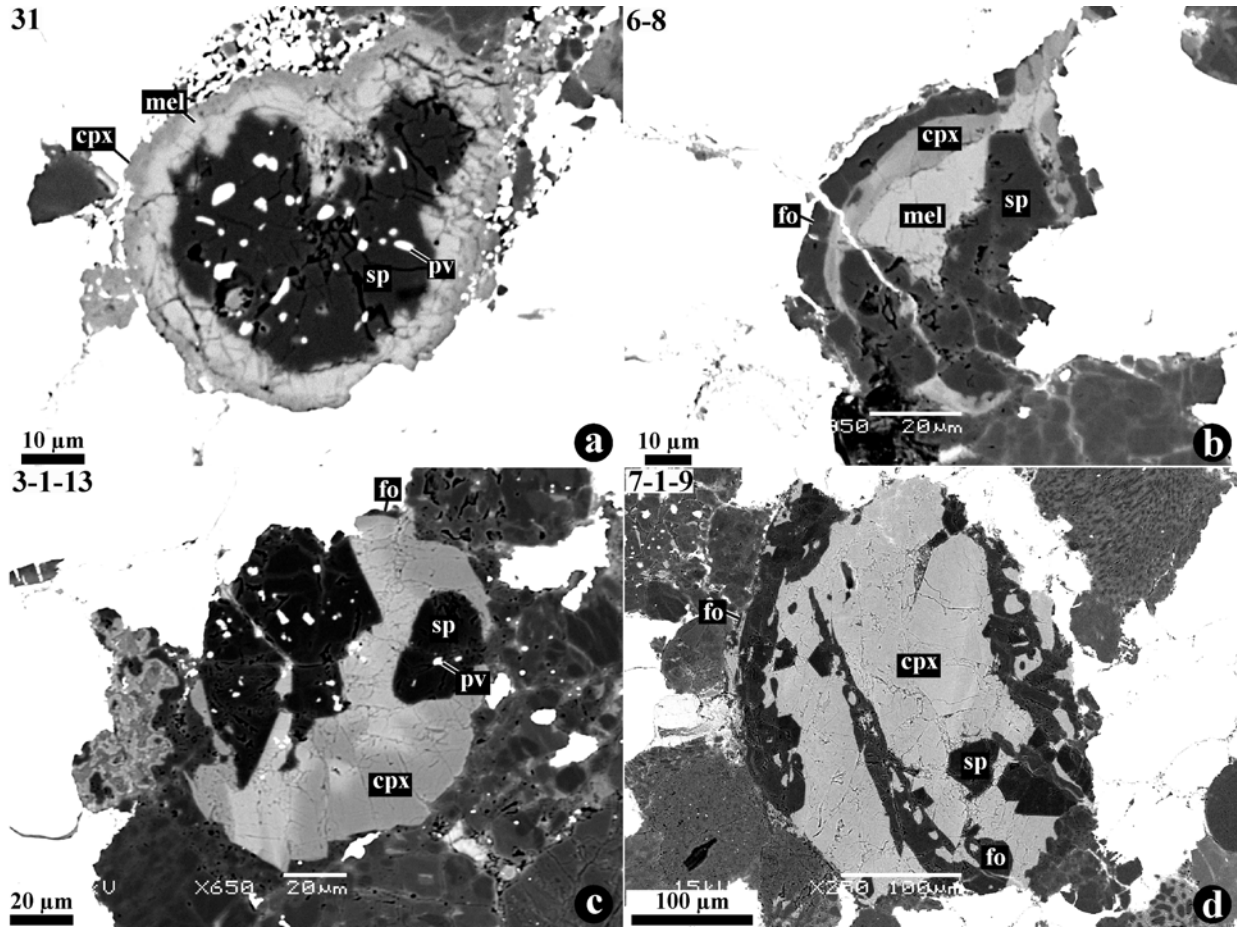

Fig. 9. BSE images of the spinel-rich CAIs. a) Irregularly shaped spinel-perovskite CAI rimmed by melilite and Al-diopside. b) Igneous CAI composed of coarse spinel grains, Al-diopside and melilite. The CAI is rimmed by a monomineralic layer of forsterite. c) Igneous CAI composed of Al-diopside and coarse spinel grains with perovskite inclusions; it is rimmed by forsterite. d) Igneous CAI or Al-rich chondrule composed of Al-diopside, spinel and forsterite and rimmed by forsterite. Pyroxenes in CAIs *6-8, 3-1-13,* and *7-1-9* show large compositional variations visible in compositional contrast. a–d) Metal-poor lithology.

DISCUSSION

The Origin of the Metal-Rich and Metal-Poor Lithologies in Isheyevo

Bulk chemical and oxygen isotopic compositions of Isheyevo are in the range of CH and CB chondrites; bulk nitrogen isotopic composition is highly enriched in ^{15}N ($\delta^{15}N \sim 1120‰$), similar to Bencubbin (CB_a) and ALH 85085 (CH) (Ivanova et al. 2008). Contrary to the known metal-rich CH and CB chondrites, however, Isheyevo consists of lithologies with variable abundances of Fe,Ni-metal and chondrules (Fig. A1). We have previously shown that inspite of the significant variations in modal mineralogy between the lithologies, they contain similar components–non-porphyritic and porphyritic ferromagnesian (type I and type II), silica-rich, and aluminum-rich chondrules, heavily hydrated (CI-like) lithic clasts and abundant (~20%) zoned Fe,Ni-metal grains (Krot et al. 2008a). Here we show that there are no systematic differences in mineralogy of CAIs and AOAs in the metal-rich and metal-poor lithologies. All types of refractory inclusions described above are found in both lithologies (Figs. 1–10). Our detailed X-ray elemental mapping of ~30 cm^2 of Isheyevo revealed no clasts composed of the metal-rich or metal-poor lithologies; the boundaries between the lithologies are typically gradational (Fig. A1). Based on these observations, we infer that the Isheyevo metal-rich and metal-poor lithologies do not represent fragments of the CB_b and CH chondrites (although the abundances of metal grains in these lithologies are similar to those in CB and CH chondrites); instead, they may have resulted from size-sorting of similar components during accretion of the Isheyevo parent body.

The observed variations in sizes and modal abundances of metal and chondrules in Isheyevo are unique among ordinary, enstatite, and non-metal-rich carbonaceous chondrites, which generally have relatively narrow range in sizes of chondrules and metal grains (e.g., Krot et al. 2003; Scott and Krot 2003 and references therein). At the same time, both groups of metal-rich chondrites, CH and CB,

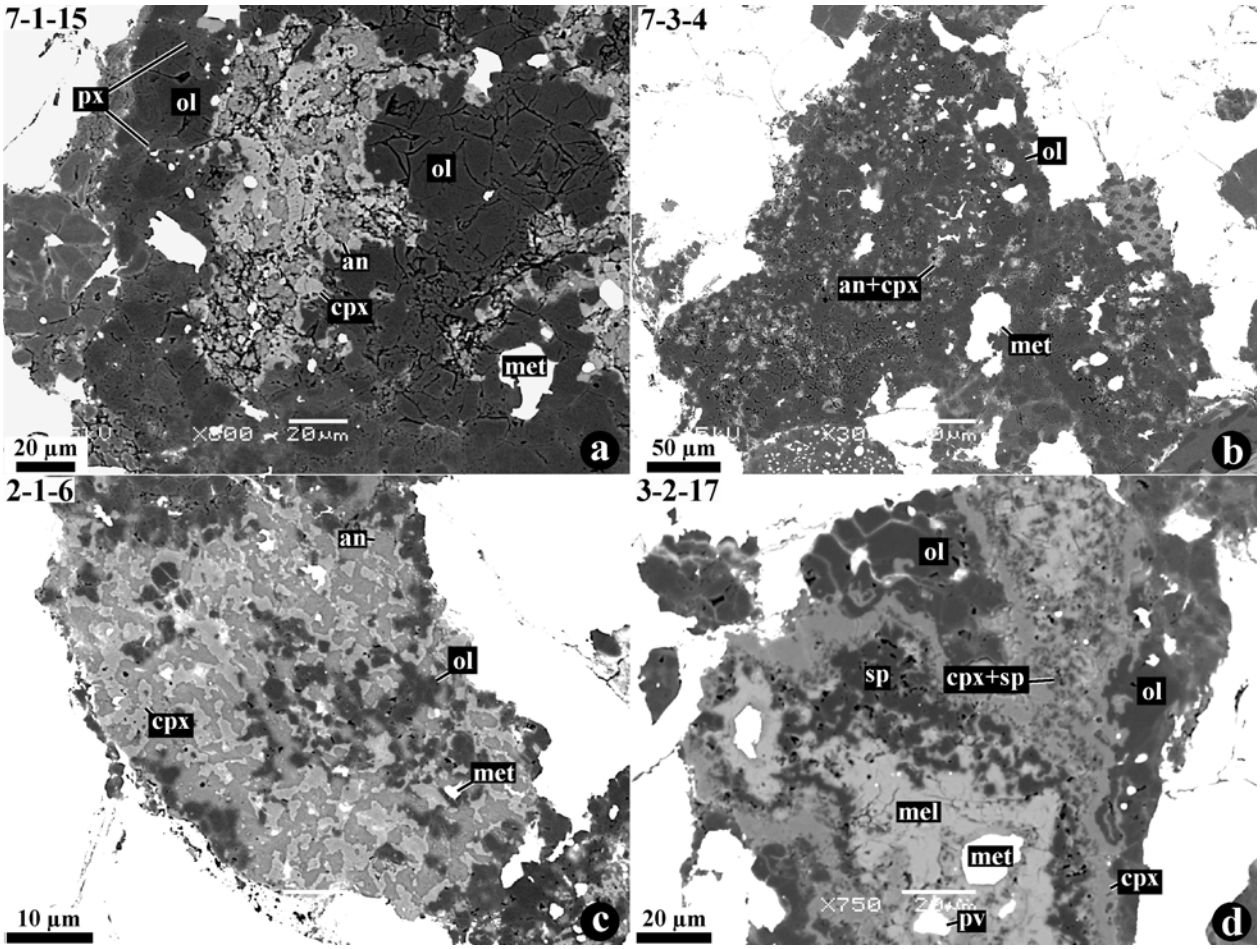

Fig. 10. BSE images of amoeboid olivine aggregates (AOAs) (a–c) and a CAI surrounded by forsterite-rich accretionary rim. a–c) AOAs composed of forsterite, Fe,Ni-metal, and a refractory component consisting of Al-diopside, anorthite, and spinel. Forsterite of AOA *7-1-5* is replaced by low-Ca pyroxene (px). AOA *2-1-6* appears to have been melted. d) Melilite-spinel-rich CAI surrounded by a thick layer of Al-diopside and a forsterite-rich accretionary rim. Melilite is replaced by a fine-grained mixture of Al-diopside and spinel. a) Metal-poor lithology; b–d) metal-rich lithology.

show large variations in metal and chondrule abundances and sizes. For example, Acfer 182 is three times coarser grained than ALH 85085 (Bischoff et al. 1993); CB_b chondrites are much fine-grained than CB_a chondrites (Weisberg et al. 2001; Krot et al. 2002a), although both subgroups appear to have formed contemporaneously (Krot et al. 2005a). These observations may indicate that size sorting played a very important role during accretion of the metal-rich chondrite parent bodies and raise a possibility of a genetic relationship between CH and CB chondrites, which we will discuss below.

Multiple Populations of Refractory Inclusions in Isheyevo and CH Chondrites?

About 55% of the Isheyevo CAIs are small (20–240 µm; average size ~80 µm; Fig. A5), compact, rounded or ellipsoidal objects dominated by very refractory minerals–hibonite, grossite, perovskite, gehlenitic melilite, spinel and Ca-Tschermake-rich pyroxenes; anorthite and Al-diopside replacing melilite are very minor or absent. Most of these CAIs appear to have igneous textures and have either poorly developed Wark-Lovering rim sequence composed of the very thin Al-diopside or melilite + Al-diopside layers, or lack the rims. The melilite rims are commonly observed around grossite-rich inclusions, whereas thin Al-diopside layers occur around melilite-rich CAIs, indicating limited high-temperature interaction with the nebular gas:

$$CaAl_4O_{7(s)} + 3Ca_{(g)} + 2SiO_{(g)} + 5H_2O_{(g)} \rightarrow 2Ca_2Al_2SiO_{7(s)} + 5H_{2(g)} \quad (1)$$

$$Ca_2MgSi_2O_{7(s)} + 2SiO_{(g)} + Mg_{(g)} + 3H_2O_{(g)} \rightarrow 2CaMgSi_2O_{6(s)} + 3H_{2(g)}. \quad (2)$$

Based on these observations, we infer that the vast majority of very refractory inclusions (pyroxene-hibonite-,

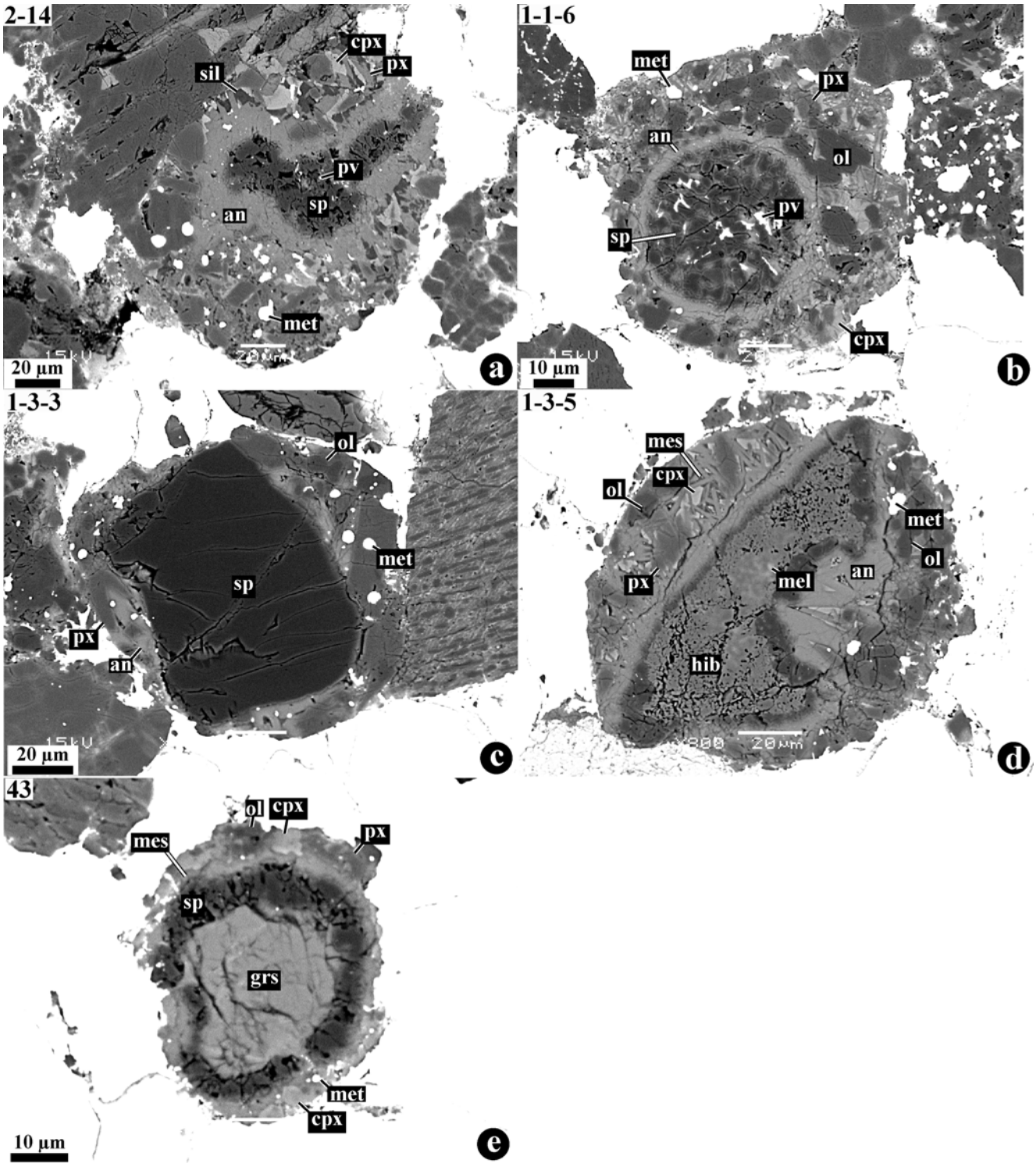

Fig. 11. BSE images of relict CAIs inside chondrules. a) Spinel-perovskite CAI surrounded by a layer of anorthite and a chondrule-like, igneous material of low-Ca pyroxene, high-Ca pyroxenes, Fe,Ni-metal, and silica. b) Rounded spinel-perovskite CAI surrounded by a layer of anorthite and a thick igneous shell of chondrule-like material of olivine, low-Ca pyroxene, high-Ca pyroxene, Fe,Ni-metal, and lath-shaped anorthitic plagioclase. c) Coarse spinel grain rimmed by an igneous layer of anorthite, low-Ca pyroxene, and Fe,Ni-metal. d) Hibonite-melilite CAI rimmed by spinel, anorthitic plagioclase and chondrule-like, igneous material of olivine, low-Ca pyroxene, high-Ca pyroxene, Fe,Ni-metal, lath-shaped anorthitic plagioclase and glassy mesostasis. e) Grossite CAI rimmed by spinel, plagioclase-normative mesostasis and an igneous layer of forsteritic olivine, low-Ca pyroxene, and high-Ca pyroxene; all phases in the igneous rim contain tiny nodules of Fe,Ni-metal. mes = mesostasis. a, b, d, e) Metal-rich lithology; c) metal-poor lithology.

hibonite-melilite-, and grossite-rich) in Isheyevo were relatively quickly and efficiently isolated from the high-temperature nebular region, prior to condensation of anorthite and forsterite, or the CAI-forming region itself cooled relatively rapidly. The latter appears to be generally consistent with disequilibrium, quenched mineral assemblages of many CH CAIs (e.g., Petaev et al. 2001b). Only few of these refractory CAIs surrounded by thick Al-diopside and forsterite rims (e.g., Fig. 2c) appear to have either stayed longer in the high-temperature nebular region or were re-introduced into this region at lower temperatures. We note, however, since there are no experimental data on the kinetics of the reactions between CAI minerals and nebular gas, this interpretation is purely qualitative.

Less refractory inclusions–CAIs composed of melilite, pyroxene, and spinel, and AOAs–comprise ~45% of refractory objects in Isheyevo. These CAIs are commonly surrounded by thick rims of Al-diopside and ±forsterite, and show clear evidence for interaction with nebular gas at relatively low temperature resulting in replacement of melilite by a fine-grained mixture of spinel, Al-diopside and ±anorthite:

$$Ca_2Al_2SiO_{7(s)} + 3SiO_{(g)} + 3Mg_{(g)} + 6H_2O_{(g)} \rightarrow 2CaMgSi_2O_{6(s)} + MgAl_2O_{4(s)} + 6H_{2(g)} \quad (3)$$

$$Ca_2Al_2SiO_{7(s)} + 3SiO_{(g)} + Mg_{(g)} + 4H_2O_{(g)} \rightarrow CaAl_2Si_2O_{8(s)} + CaMgSi_2O_{6(s)} + 4H_{2(g)} \quad (4)$$

Forsterite in some AOAs is replaced by low-Ca pyroxene:

$$Mg_2SiO_{4(s)} + SiO_{(g)} + H_2O_{(g)} \rightarrow 2MgSiO_{3(s)} + H_{2(g)}. \quad (5)$$

These observations may indicate that there are at least two populations of refractory inclusions in Isheyevo: a population of very refractory, rounded CAIs largely composed of hibonite, grossite, perovskite, gehlenitic melilite, spinel and Ca-Tschermake-rich pyroxenes and a population of less refractory CAIs and AOAs dominated by more åkermanitic melilite, Al-diopside, spinel, anorthite, and forsterite. The existence of multiple populations of CAIs in Isheyevo can be potentially tested by detailed oxygen and magnesium isotopic measurements. If these CAIs formed in different nebular regions or at different times, they may show the differences in the initial $^{26}Al/^{27}Al$ ratios and/or oxygen isotopic compositions.

Our preliminary results on oxygen and aluminum-magnesium isotope systematics of the Isheyevo CAIs appear to support the existence of two populations of refractory inclusions in this meteorite: one with the canonical $^{26}Al/^{27}Al$ ratios of ~5×10^{-5} and another with either unresolvable excesses of ^{26}Mg ($^{26}Mg^*$) or with $^{26}Mg^*$ corresponding to the $^{26}Al/^{27}Al$ ratio of ~4×10^{-7}; both populations are characterized by ^{16}O-rich compositions (Krot et al. 2007, 2008b). We note, however, that more work is needed to confirm this hypothesis.

Oxygen and aluminum-magnesium isotopic systematics of CAIs in CH chondrites may also suggest the presence of at least two populations of refractory inclusions in CH chondrites (MacPherson et al. 1989; Kimura et al. 1993; Weber et al. 1995a; Sahijpal et al. 1999). Five out of 33 CH CAIs have large excesses of ^{26}Mg ($^{26}Mg^*$) corresponding to $^{26}Al/^{27}Al$ ratios of ~5×10^{-5}, whereas others (most of them are hibonite- and grossite-rich CAIs similar to those in Isheyevo) show no resolvable $^{26}Mg^*$ (MacPherson et al. 1989; Kimura et al. 1993; Weber et al. 1995a; Sahijpal et al. 1999). Sahijpal et al. (1999) reported a bi-modal distribution of oxygen isotopic compositions of CH CAIs; most hibonite- and grossite-rich CAIs are ^{16}O-rich, whereas most pyroxene-spinel-rich, igneous CAIs are ^{16}O-depleted.

Comparison of the Isheyevo Refractory Inclusions with Those in Other Chondrite Groups

A population of very refractory inclusions in Isheyevo largely composed of grossite, hibonite, gehlenitic melilite, and Al-diopside (Figs. 1–4), is texturally and mineralogically most similar to the majority of CAIs in the previously studied CH chondrites Acfer 182, ALH 85085, PCA 91467, NWA 470, NWA 739, and NWA 770 (MacPherson et al. 1989; Kimura et al. 1993; Weber et al. 1995a, 1995b; Krot et al. 1999a, 1999b, 2002a, 2006a; Ivanova et al. 2001, 2002). Oxygen and magnesium isotopic compositions of these CAIs reported by Krot et al. (2007, 2008b) support this conclusion: most of them are ^{16}O-rich and have small or unresovlable excesses of ^{26}Mg.

The mineralogy, textures, and sizes of the very refractory population of the Isheyevo CAIs are quite distinct from those of CAIs in the CR (Weber and Bischoff 1997; Aléon et al. 2002), CO (e.g., Russell et al. 1998), CM, and CV chondrites (MacPherson et al. 1988 and references therein) and ungrouped carbonaceous chondrites Acfer 094 (Krot et al. 2004c), Adelaide (Huss et al. 2003), and MAC 87300 and MAC 88107 (Russell et al. 2000a). Although grossite- and hibonite-rich CAIs have been reported in different chondrite groups (e.g., MacPherson 2003 and references therein), the dominant inclusion types in most chondrite groups are spinel-pyroxene ± melilite CAIs and AOAs; igneous CAIs are generally rare (coarse-grained Type A, B, and C CAIs in CV chondrites are exceptions) (Lin et al. 2006).

The population of less refractory Isheyevo inclusions (Figs. 5a–c, 6–8, 9a, 10) is texturally and mineralogically similar to CAIs in other chondrite groups (MacPherson 2003 and references therein; Lin et al. 2006), which commonly show evidence for gas-solid condensation reactions, resulting in replacement of high-temperature minerals by the low-temperature mineral assemblages; e.g., replacement of melilite and spinel by anorthite and Al-diopside (e.g., Krot et al. 2004d), and replacement of forsterite by low-Ca pyroxene (Krot et al. 2004a, 2004b).

Some of the spinel-pyroxene, igneous Isheyevo CAIs (Figs. 9b–d) are mineralogically similar to those in the CB_b chondrites (HaH 237 and QUE 94411, QUE 94627), which are dominated by the spinel-pyroxene ± melilite igneous CAIs surrounded by forsterite rims (see Figs. 2a, 2c, 5, 6 in Krot et al. 2001b). Oxygen or magnesium isotopic compositions of these CAIs have yet to be reported.

The observations that majority of CAIs in Isheyevo are similar to those in metal-rich (CH and CB) chondrites and distinct from those in other chondrite groups suggest that either CAIs in metal-rich and other chondrite groups originated in different nebular regions with distinct physical-chemical conditions or CAI formation occurred multiple times under a distinct set of physical-chemical conditions (e.g., dust/gas ratio, peak heating temperature, cooling rate, ambient temperature, isolation temperature, and number of recycling episodes) in a localized nebular region followed by dispersal around the proto-Sun. The latter hypothesis is generally consistent with the X-wind astrophysical setting for the formation of CAIs (Shu et al. 1996). The observations that majority of Isheyevo CAIs are mineralogically similar to those in CH and CBb chondrites may provide an evidence for a genetic relationship between these chondrite groups as discussed below.

Implication for a Possible Genetic Relationship between CH and CB Chondrites

Wasson and Kallemeyn (1990) first suggested that CH chondrite ALH 85085 contains two kinds of materials: one produced by nebular processes and one produced during collision between asteroids. The former include refractory inclusions and porphyritic chondrules; the latter include magnesian cryptocrystalline chondrules. Subsequently Rubin et al. (2003) and Campbell et al. (2002) proposed an impact origin of metal ± sulfide and silicate nodules (chondrules) in the CB_a chondrites Gujba, Weatherford, and Bencubbin.

Based on the young ^{207}Pb-^{206}Pb ages of chondrules in CB_a and CB_b chondrites and mineralogical observations (e.g., presence of only magnesian, non-porphyritic chondrules and lack of evidence for recycling of chondrules and zoned metal condensates), Krot et al. (2005a) concluded that magnesian cryptocrystalline and skeletal chondrules and metal grains in these meteorites formed late, by a single-stage process, most likely in an impact generated plume during collision between planetary embryos. Subsequently, Krot et al. (2006d) suggested that the magnesian cryptocrystalline chondrules, which are highly depleted in Ca, Al, and REE (down to $<0.01 \times$ CI), condensed directly from the plume, whereas the magnesian skeletal chondrules, which are commonly rich in Ca, Al, and REE (up to $10 \times$ CI), represent melt fraction of the plume.

Based on the mineralogy and petrography of chondrules in Isheyevo, Krot et al. (2008a) concluded, that there are at least two populations of chondrules in this meteorite, which may have formed by different mechanisms. The first population of chondrules includes magnesian cryptocrystalline and skeletal chondrules, which are similar to those in CB_b and CH chondrites. Such chondrules are virtually absent in other chondrite groups and could have formed by a similar process, i.e., in an impact-generated plume produced by collision of planetary embryos (Krot et al. 2005a, 2008a). The second population of chondrules includes ferromagnesian (type I and type II), silica-rich and Al-rich chondrules with porphyritic textures which probably formed by melting of dust, including CAIs (Fig. 11), like most chondrules in different chondrite groups (Krot et al. 2008a).

The mineralogy and petrography of the Isheyevo CAIs (this study) as well as their oxygen and magnesium isotopic compositions (Krot et al. 2007, 2008b) also indicate that these CAIs are similar to those in CH and CB_b chondrites.

Based on these observations, we infer that Isheyevo, as well as other metal-rich carbonaceous chondrites (CH, CB_a and CB_b), consist of different proportions of materials produced by three different processes: 1) in an impact generated plume (magnesian cryptocrystalline and skeletal chondrules and zoned metal grains; some ^{16}O-depleted igneous CAIs could have been melted during this event), 2) by evaporation, condensation, and melting of dust in the protoplanetary disk (porphyritic chondrules and refractory inclusions), and 3) by aqueous alteration of pre-existing planetesimals (heavily hydrated lithic clasts). The CB_a and CB_b chondrites consist almost entirely of the impact generated materials, whereas CH chondrites contain higher proportion of components produced in the solar nebula. In contrast to CH chondrites, Isheyevo consists of lithologies with different proportions of nebular and asteroidal materials. These differences are probably due to size sorting during accretion into the Isheyevo parent body. It is unclear at this point, whether the hypothetical impact proposed to explain the origin of the magnesian cryptocrystalline and skeletal chondrules and metal grains in CBs, CHs, and Isheyevo was the same or there were multiple events. To answer this question, detailed studies of trace element abundances, O-, Al-Mg and Pb-Pb isotopic systematics of chondrules are required.

Are any of the Isheyevo CAIs Condensed from an Impact-Generated Plume?

Since grossite- and hibonite-rich CAIs are dominant in Isheyevo and other CH chondrites and very rare in other chondrite groups, is it possible that a population of this very refractory, probably igneous CAIs in Isheyevo, which appear to have cooled very rapidly, condensed as liquid droplets from a plume produced during a hypothetical asteroidal collision?

Our preliminary studies (Krot et al. 2007, 2008b) indicate that most CAIs in Isheyevo, including hibonite-rich and grossite-rich types, have uniformly ^{16}O-rich compositions ($\Delta^{17}O < -20‰$), like most CAIs in primitive

chondrites (Scott and Krot 2003 and references therein), suggesting formation in the presence of ^{16}O-rich nebular gas. In contrast, magnesian cryptocrystalline and skeletal olivine-pyroxene chondrules (presumably of impact origin) have ^{16}O-poor compositions ($\Delta^{17}O > -5‰$), indicating that they formed from an isotopically distinct reservoir (Krot et al. 2007).

We note that rare CAIs found in CB_b chondrites have ^{16}O-depleted ($\Delta^{17}O$ from −12 to −5‰) relative to typical CAIs ($\Delta^{17}O < -20‰$) compositions (Krot et al. 2001a), show mass-dependent fractionation of Mg isotopes and no evidence for excesses of ^{26}Mg (Gounelle et al. 2006), and are characterized by group I rare earth element (REE) patterns (10–100 × CI and negative Eu, Ce, and Yb anomalies) (Russell et al. 2000b). In contrast, chondrules of presumably impact origin in CB_b chondrites have flat REE patterns (<0.01 to 10 × CI) and more ^{16}O-depleted compositions ($\Delta^{17}O$ from 7 to 2‰). We infer that CAIs in CB_b chondrites did not condense from the impact generated plume, but could have been melted during this event and experienced extensive oxygen and magnesian isotopic exchange, and, possibly, evaporation.

Our observations summarized in section 3.3 indicate that some of the Isheyevo CAIs, including hibonite-rich and grossite-rich, experienced remelting in the chondrule-forming region. This process resulted in formation of 1) igneous rims of ferromagnesian chondrule-like material around CAIs (Fig. 11e), 2) Type C CAIs intergrown with chondrule-like minerals (e.g., ferromagnesian olivine and low-Ca pyroxene, Figs. 7c–f), and 3) relict CAIs inside porphyritic chondrules (Figs. 11a–d). Based on these observations, we infer that formation of Isheyevo CAIs predates formation of porphyritic chondrules (presumably of non-impact origin) in this meteorite. We note that neither magnesian, non-porphyritic chondrules nor metal grains which could have been produced during a hypothetical collision event show evidence for remelting (Krot et al. 2005a). In fact, this is one of the main arguments in favor of impact origin of the CB chondrules and metal grains (Krot et al. 2005a).

Based on these observations, we infer that it is highly unlikely that Isheyevo CAIs condensed during the hypothesized asteroidal collision that may have resulted in formation of magnesian non-porphyritic chondrules and Fe,Ni-metal grains in the metal-rich carbonaceous chondrites (Krot et al. 2005a, 2008a). We note, however, that some of the igneous spinel-pyroxene CAIs appear to have experienced very fast cooling during solidification, indicated by the chondrule-like, radial (Fig. 1d) or skeletal textures (Fig. 9d). Such textures are not typical for CAIs (e.g., MacPherson et al. 1988; MacPherson 2003 and references therein) and may indicate that these CAIs were melted in the chondrule-forming region without addition of chondrule-like precursors. The melting may have occurred either during impact plume-generated event (Krot et al. 2005a) or during melting of "normal" chondrules, possibly by shock wave (Desch et al. 2006 and references therein). Since chondrules formed in the presence of ^{16}O-poor nebular gas (Krot et al. 2006c and references therein), future oxygen isotopic studies of these CAIs may provide a possible test of this hypothesis.[1]

CONCLUSIONS

1. The CH/CB-like carbonaceous chondrite Isheyevo consists of Fe,Ni-metal grains, chondrules, refractory inclusions, and heavily hydrated matrix lumps. There are significant variations in size and relative abundance of Fe,Ni-metal (90, 70, 20, and 7 vol%) and chondrules, as well as proportions of porphyritic versus non-porphyritic chondrules between different portions of Isheyevo, which we called "lithologies." We described the mineralogy and petrography of CAIs and AOAs in the metal-rich (~70 vol% Fe,Ni-metal) and metal-poor (~20 vol% Fe,Ni-metal) lithologies.
2. Based on the major mineralogy, ~330 refractory inclusions studied in ~30 cm^2 of polished are of Isheyevo are divided into hibonite ± pyroxene ± melilite ± spinel (39%), grossite-rich (16%), melilite-rich (19%), spinel-rich (14%), pyroxene-anorthite-rich (8%), fine-grained spinel-rich CAIs (1%), and AOAs (4%). All types of refractory inclusions are mineralogically pristine and show no evidence for iron-alkali metasomatic alteration, hydration, or thermal metamorphism.
3. There are no systematic differences in the inclusion types or their relative abundances between the lithologies. These observations as well as the lack of mineralogical differences in chondrules and metal grains between the lithologies and the lack of clasts composed of different lithologies may indicate that the lithologies resulted from size sorting of similar components during accretion in the Isheyevo parent body; they do not represent fragments of CH and CB chondritic materials.
4. It appears that there are two populations of refractory inclusions in Isheyevo:
   a) About 55% of the CAIs are very refractory (hibonite-rich and grossite-rich), compact, rounded or ellipsoidal objects, 20–240 μm in apparent diameter, which appear to have crystallized from rapidly cooling melts. These CAIs generally lack minerals produced as a result of gas-solid condensation reactions at relatively low temperatures (below ~1350 K), such as anorthite and forsterite. These

[1]Our preliminary results supports this hypothesis: two coarse-grained, igneous, spinel-pyroxene CAIs surrounded by forsterite rims are ^{16}O-depleted ($\Delta^{17}O \sim -10‰$) compared to typical, ^{16}O-rich ($\Delta^{17}O < -20‰$) CAIs (Krot et al. 2008b).

observations may indicate that these CAIs experienced limited interaction with the nebular gas below 1350 K, suggesting either a short residence time in the CAI-forming region or the CAI-forming region itself cooled rapidly. These CAIs are texturally and mineralogically similar to the majority of CAIs in the previously studied CH chondrites (Acfer 182, ALH 85085, PCA 91467, PAT 91546, NWA 470, NWA 739, and NWA 770), and, to a less degree, to those in the CB_b chondrites (HaH 237, QUE 94411, and QUE 94627). They are distinctly different from CAIs in other carbonaceous chondrite groups (CR, CM, CV, CK, CO) and ungrouped carbonaceous chondrites Acfer 094, Adelaide, MAC 87300, and MAC 88107, which are dominated by the spinel-pyroxene ± melilite CAIs and AOAs.

b) The remaining 45% of refractory inclusions are less refractory objects (melilite-, spinel- and pyroxene-rich CAIs and AOAs), 40–300 μm in apparent diameter, which are texturally and mineralogically similar to those in other chondrite groups. Many of these CAIs and AOAs appear to have experienced more extensive interaction with nebular gas resulting in replacement of melilite and spinel by anorthite and Al-diopside, and of forsterite by low-Ca pyroxene, and formation of the relatively thick Wark-Lovering rim layers of Al-diopside and forsterite. The pyroxene-spinel, igneous CAIs surrounded by forsterite rims are texturally and mineralogically similar to those in CB_b chondrites.

5. CAIs of both populations are found as relict inclusions inside porphyritic chondrules, indicating that they experienced recycling during chondrule formation. Although some of the Isheyevo CAIs could have been melted in an impact-generated plume during hypothesized collision between planetary embryos that produced magnesian cryptocrystalline and skeletal chondrules and metal grains in CB and, possibly, CH chondrites, there is no evidence that any CAIs in Isheyevo condensed from this plume.
6. We suggest that Isheyevo, as well as other metal-rich carbonaceous chondrites (CH, CB_a, and CB_b), consist of variable proportions of materials produced by different processes in different settings: 1) by evaporation, condensation, and melting of dust in the protoplanetary disk (porphyritic chondrules and refractory inclusions), 2) by melting, evaporation and condensation in an impact-generated plume (magnesian cryptocrystalline and skeletal chondrules and metal grains; some igneous CAIs could have been melted during this event), and 3) by aqueous alteration of pre-existing planetesimals (heavily hydrated lithic clasts). The CB_a and CB_b chondrites consist almost entirely of the impact-generated materials, whereas CH chondrites contain higher proportion of components produced in the solar nebula. In contrast to CH chondrites, Isheyevo contains lithologies with different proportions of nebular and asteroidal materials.

Acknowledgments—We thank Drs. T. Fagan and Y. Lin for detailed reviews and numerous suggestions which helped to improve the manuscript. We thank Dr. H. Nagahara (associate editor) for her patience and detailed comments. This work was supported by NASA grants NAG5-10610 (A. N. Krot, P. I.), and NAG5-4212 (K. Keil, P. I.). This is Hawai'i Institute of Geophysics and Planetology Publication no. 1701 and School of Ocean and Earth Science and Technology Publication no. 7583.

Editorial Handling—Dr. Hiroko Nagahara

REFERENCES

Aléon J., Krot A. N., and McKeegan K. D. 2002. Ca-Al-rich inclusions and amoeboid olivine aggregates from the CR carbonaceous chondrites. *Meteoritics & Planetary Science* 37: 1729–1755.

Bischoff A. and Keil K. 1984. Al-rich objects in ordinary chondrites: Related origin of carbonaceous and ordinary chondrites and their constituents. *Geochimica et Cosmochimica Acta* 48:693–709.

Bischoff A., Palme H., Schultz L., Weber D., Weber H., and Spettel B. 1993. Acfer 182 and paired samples, an iron-rich carbonaceous chondrite: Similarities with ALH 85085 and relationship to CR chondrites. *Geochimica et Cosmochimica Acta* 57:2631–2648.

Campbell A. J., Humayun M., Meibom A., Krot A. N., and Keil K. 2001. Origin of zoned metal in the QUE 94411 chondrite. *Geochimica et Cosmochimica Acta* 65:163–180.

Campbell A. J., Humayun M., and Weisberg M. K. 2002. Siderophile element constraints on the formation of metal in the metal-rich chondrites Bencubbin, Weatherford, and Gujba. *Geochimica et Cosmochimica Acta* 66:647–660.

Campbell A. J. and Humayun M. 2004. Formation of metal in the CH chondrites ALH 85085 and PCA 91467. *Geochimica et Cosmochimica Acta* 68:3409–3422.

Desch S. J., Ciesla F. J., Hood L. L., and Nakamoto T. 2005. Heating of chondritic materials in solar nebula shocks. In *chondrules and the protoplanetary disk*, edited by Krot A. N., Scott E. R. D., and Reipurth B. Astronomical Society of the Pacific Conference Series, vol. 341. pp. 851–885.

Gounelle M., Young E. D., Shahar A., and Kearsley A. 2006. Magnesium isotopic composition of CAIs and chondrules from CB_b chondrites (abstract #2014). 37th Lunar and Planetary Science Conference. CD-ROM.

Grossman J. N., Rubin A. E., and MacPherson G. J. 1988. ALH 85085; a unique volatile-poor carbonaceous chondrite with possible implications for nebular fractionation processes. *Earth and Planetary Science Letters* 91:33–54.

Huss G. R., Hutcheon I. D., Krot A. N., and Tachibana S. 2003. Oxygen isotopes in refractory inclusions from the Adelaide carbonaceous chondrite (abstract). 34th Lunar and Planetary Science Conference. CD-ROM. #1802.

Ivanova M. A., Petaev M. I., Nazarov M. A., Taylor A. L., and Wood J. A. 2001. Refractory inclusions from the new CH, NWA 470 (abstract #1392). 32nd Lunar and Planetary Science Conference. CD-ROM.

Ivanova M. A., Petaev M. I., MacPherson G. J., Nazarov M. A., Taylor L. A., and Wood J. A. 2002. The first known natural

occurrence of calcium monoaluminate, in a calcium-aluminum-rich inclusion from the CH chondrite Northwest Africa 470. *Meteoritics & Planetary Science* 37:1337–1344.

Ivanova M. A., Kononkova N. N., Greenwood R. C., Franchi I. A., Krot A. N., Verchovsky A. B., Trieloff M., Korochantseva E. V., and Brandstätter F. 2008. The Isheyevo meteorite: Mineralogy, petrography, bulk chemistry, oxygen, nitrogen, carbon isotopic compositions, and ^{40}Ar-^{39}Ar ages. *Meteoritics & Planetary Science* 43:915–941.

Kimura M., El Goresy A., Palme H., and Zinner E. 1993. Ca-, Al-rich inclusions in the unique chondrite ALH 85085: Petrology, chemistry, and isotopic compositions. *Geochimica et Cosmochimica Acta* 57:2329–2359.

Kobayashi S., Imai H., and Yurimoto H. 2003. New extreme ^{16}O-rich reservoir in the early solar system. *Geochemical Journal* 37:663–669.

Krot A. N. and Keil K. 2002. Anorthite-rich chondrules in CR and CH carbonaceous chondrites: Genetic link between Ca, Al-rich inclusions and ferromagnesian chondrules. *Meteoritics & Planetary Science* 37:91–111.

Krot A. N., Sahijpal S., McKeegan K. D., Weber D., Ulyanov A. A., Petaev M. I., Meibom A., and Keil K. 1999a. Unique mineralogy and isotopic signatures of calcium-aluminum-rich inclusions from the CH chondrite Acfer 182 (abstract). *Meteoritics & Planetary Science* 34:A69.

Krot A. N., Ulyanov A. A., and Weber D. 1999b. Al-diopside-rich refractory inclusions in the CH chondrite Acfer 182 (abstract #2018). 30th Lunar and Planetary Science Conference. CD-ROM.

Krot A. N., Meibom A., and Keil K. 2000. Volatile-poor chondrules in CH carbonaceous chondrites: Formation at high ambient nebular temperature (abstract #1481). 31st Lunar and Planetary Science Conference. CD-ROM.

Krot A. N., Meibom A., Russell S. S., Alexander C. M. O'D, Jeffries T. E., and Keil K. 2001a. A new astrophysical setting for chondrule formation. *Science* 291:1776–1779.

Krot A. N., McKeegan K. D., Russell S. S., Meibom A., Weisberg M. K., Zipfel J., Krot T. V., Fagan T. J., and Keil K. 2001b. Refractory Ca,Al-rich inclusions and Al-diopside-rich chondrules in the metal-rich chondrites Hammadah al Hamra 237 and QUE 94411. *Meteoritics & Planetary Science* 36:1189–1217.

Krot A. N., Ulyanov A. A., Meibom A., and Keil K. 2001c. Forsterite-rich accretionary rims around Ca,Al-rich inclusions from the reduced CV3 chondrite Efremovka. *Meteoritics & Planetary Science* 36:611–628.

Krot A. N., Hutcheon I. D., and Huss G. R. 2001d. Aluminum-rich chondrules and associated refractory inclusions in the unique carbonaceous chondrite Adelaide (abstract). *Meteoritics & Planetary Science* 36:A105–A107.

Krot A. N., Huss G. R., and Hutcheon I. D. 2001e. Corundum-hibonite refractory inclusions from Adelaide: Condensation or crystallization from melt? (abstract). *Meteoritics & Planetary Science* 36:A105.

Krot A. N., Meibom A., Weisberg M. K., and Keil K. 2002a. The CR chondrite clan: Implications for early solar system processes. *Meteoritics & Planetary Science* 37:1451–1490.

Krot A. N., Hutcheon I. D., and Keil K. 2002b. Anorthite-rich chondrules in the reduced CV chondrites: Evidence for complex formation history and genetic links between CAIs and ferromagnesian chondrules. *Meteoritics & Planetary Science* 37: 155–182.

Krot A. N., Keil K., Goodrich C. A., Weisberg M. K., and Scott E. R. D. 2003. Classification of meteorites. In *Meteorites, comets and planets*, edited by Davis A. M. Treatise on Geochemistry, vol. 1. Oxford: Elsevier-Pergamon. pp. 83–129.

Krot A. N., Petaev M. I., Russell S. S., Itoh S., Fagan T., Yurimoto H., Chizmadia L., Weisberg M. K., Komatsu M., Ulyanov A. A., and Keil K. 2004a. Amoeboid olivine aggregates in carbonaceous chondrites: Records of nebular and asteroidal processes. *Chemie der Erde* 64:185–239.

Krot A. N., Fagan T. J., Yurimoto H., and Petaev M. I. 2004b. Origin of low-Ca pyroxene in amoeboid olivine aggregates: Evidence from oxygen isotopic compositions. *Geochimica et Cosmochimica Acta* 68:1873–1881.

Krot A. N., Fagan T. J., Keil K., McKeegan K. D., Sahijpal S., Hutcheon I. D., Petaev M. I., and Yurimoto H. 2004c. Ca, Al-rich inclusions, amoeboid olivine aggregates, and Al-rich chondrules from the unique carbonaceous chondrite Acfer 094: I. Mineralogy and petrology. *Geochimica et Cosmochimica Acta* 68:2167–2184.

Krot A. N., MacPherson G. J., Ulyanov A. A., and Petaev M. I. 2004d. Fine-grained, spinel-rich inclusions from the reduced CV chondrites Efremovka and Leoville: I. Mineralogy, petrology, and bulk chemistry. *Meteoritics & Planetary Science* 39:1517–1553.

Krot A. N., Amelin Y., Cassen P., and Meibom A. 2005a. Young chondrules in CB chondrites from a giant impact in the early solar system. *Nature* 436:989–992.

Krot A. N., Yurimoto H., Hutcheon I. D., and MacPherson G. J. 2005b. Relative chronology of CAI and chondrule formation: Evidence from chondrule-bearing igneous CAIs. *Nature* 434:998–1001.

Krot A. N., McKeegan K. D., Huss G. R., Liffman K., Sahijpal S., Hutcheon I. D., Srinivasan G., Bischoff A., and Keil K. 2005c. Aluminum-magnesium and oxygen isotope study of relict Ca-Al-rich inclusions in chondrules. *The Astrophysical Journal* 629: 1227–1237.

Krot A. N., Petaev M. I., and Keil K. 2006a. Mineralogy and petrology of Al-rich objects in the CH carbonaceous chondrite Northwest Africa 739. *Chemie der Erde* 66:57–76.

Krot A. N., Ulyanov A. A., and Ivanova M. A. 2006b. Refractory inclusions and aluminum-rich chondrules in the CB/CH-like carbonaceous chondrite Isheyevo (abstract #1226). 37th Lunar Planetary Science Conference. CD-ROM.

Krot A. N., Yurimoto H., McKeegan K. D., Leshin L., Chaussidon M., Libourel G., Yoshitake M., Huss G. R., Guan Y., and Zanda B. 2006c. Oxygen isotopic compositions of chondrules: Implications for evolution of oxygen isotopic reservoirs in the inner solar nebula. *Chemie der Erde* 66:249–276.

Krot A. N., Ulyanov A. A., Ivanova M. A., and Russell S. S. 2006d. Origins of chondrules in the metal-rich carbonaceous chondrites (abstract #1224). 37th Lunar and Planetary Science Conference. CD-ROM.

Krot A. N., Nagashima K., and Ulyanov A. A. 2007a. Oxygen isotopic compositions of calcium-aluminum-rich inclusions and chondrules in the CB/CH-like carbonaceous chondrite Isheyevo (abstract #1888). 38th Lunar and Planetary Science Conference. CD-ROM.

Krot A. N., Ivanova M. A., and Ulyanov A. A. 2008a. Chondrules in the CB/CH-like carbonaceous chondrite Isheyevo: Evidence for various chondrule-forming mechanisms and multiple chondrule generations. *Chemie der Erde* 67:283–300.

Krot A. N., Nagashima K., Bizzarro M., Huss G. R., Davis A. M., McKeegan K. D., Meyer B. S., and Ulyanov A. A. 2008b. Multiple generations of refractory inclusions in the metal-rich carbonaceous chondrites Acfer 182/214 and Isheyevo. *The Astrophysical Journal* 672:713–721.

Lin Y., Kimura M., Miao B., Dai D., and Monoi A. 2006. Petrographic comparison of refractory inclusions from different chemical groups of chondrites. *Meteoritics & Planetary Science* 41:67–83.

MacPherson G. J. 2003. Calcium-aluminum-rich inclusions in chondritic meteorites. In *Meteorites, comets, and planets*, edited

by Davis A. M. Treatise on Geochemistry, vol. 1. Oxford: Elsevier-Pergamon. pp. 201–247.

MacPherson G. J., Wark D. A., and Armstrong J. T. 1988. Primitive material surviving in chondrites: Refractory inclusions. In *Meteorites and the early solar system*, edited by Kerridge J. F. and Matthews M. S. Tucson: The University of Arizona Press. pp. 746–807.

MacPherson G. J., Davis A. M., and Grossman J. N. 1989. Refractory inclusions in the unique chondrite ALH 85085 (abstract). *Meteoritics* 24:297.

Makide K., Kobayashi S., and Yurimoto H. 2004. Aluminium-26 and oxygen isotopic distributions of Ca-Al-rich inclusions from Acfer 214 CH chondrite (abstract #9076). Workshop on Chondrites and the Protoplanetary Disk. CD-ROM.

Meibom A., Petaev M. I., Krot A. N., Wood J. A., and Keil K. 1999. Primitive FeNi metal grains in CH carbonaceous chondrites formed by condensation from a gas of solar composition. *Journal of Geophysical Research* 104:22,053–22,059.

Meibom A., Desch S. J., Krot A. N., Cuzzi J. N., Petaev M. I., Wilson L., and Keil K. 2000. Large scale thermal events in the solar nebula: Evidence from FeNi metal grains in primitive meteorites. *Science* 288:839–841.

Meibom A., Petaev M. I., Krot A. N., Keil K., and Wood J. A. 2001. Growth mechanism and additional constraints on FeNi-metal condensation in the solar nebula. *Journal of Geophysical Research* 106:32,797–32,801.

Meibom A., Krot A. N., Robert F., Mostefaoui S., Russell S. S., Petaev M. I., and Gounelle M. 2007. Nitrogen and carbon isotopic composition of the Sun inferred from a high-temperature solar nebular condensate. *The Astrophysical Journal* 656:L33–L36.

Petaev M. I., Meibom A., Krot A. N., Wood J. A., and Keil K. 2001a. The condensation origin of zoned grains in QUE 94411: Implications for the formation of the Bencubbin-like chondrites. *Meteoritics & Planetary Science* 36:93–107.

Petaev M. I., Ivanova M. A., Nazarov M. A., and Wood J. A. 2001b. Al-rich clinopyroxene in the CH chondrite NWA 470: Condensates from fractionated nebular systems (abstract #1445). 32nd Lunar and Planetary Science Conference. CD-ROM.

Rubin A. E., Kallemeyn G. W., Wasson J. T., Clayton R. N., Mayeda T. K., Grady M., Verchovsky A. B., Eugster O., and Lorenzetti S. 2003. Formation of metal and silicate globules in Gujba: A new Bencubbin-like meteorite fall. *Geochimica et Cosmochimica Acta* 67:3283–3298.

Russell S. S., Huss G. R., Fahey A. J., Greenwood R. C., Hutchison R., and Wasserburg G. J. 1998. An isotopic and petrologic study of calcium-aluminum-rich inclusions from CO3 meteorites. *Geochimica et Cosmochimica Acta* 62:689–714.

Russell S. S., Davis A. M., MacPherson G. J., Guan Y., Huss G. R. 2000a. Refractory inclusions from the ungrouped carbonaceous chondrites MAC 87300 and MAC 88107. *Meteoritics & Planetary Science* 35:1055–1066.

Russell S. S., Krot A. N., Meibom A., Alexander C. M. O'D., and Jeffries T. E. 2000b. Chondrules of the first generation? Trace element geochemistry of silicate from Bencubbin/CH-like meteorites (abstract). *Meteoritics & Planetary Science* 35: A139.

Russell S. S., Krot A. N., MacPherson G. J., Huss G. R., Itoh S., Yurimoto H., and Keil K. 2005. Genetic relationship between refractory inclusions and chondrules. In *Chondrules and the protoplanetary disk*, edited by Krot A. N., Scott E. R. D., and Reipurth B. Astronomical Society of the Pacific Conference Series, vol. 341. pp. 317–353.

Sahijpal S., McKeegan K. D., Krot A. N., Weber D., and Ulyanov A. A. 1999. Oxygen isotopic compositions of calcium-aluminum-rich inclusions from the CH chondrites, Acfer 182 and PAT 91546 (abstract). *Meteoritics & Planetary Science* 34:A101.

Scott E. R. D. 1988. A new kind of primitive chondrite, Allan Hills 85085. *Earth and Planetary Science Letters* 91:1–18.

Scott E. R. D. and Krot A. N. 2003. Chondrites and their components. In *Meteorites, comets and planets*, edited by Davis A. M. Treatise on Geochemistry, vol. 1. Oxford: Elsevier-Pergamon. pp. 143–200.

Shu F. H., Shang H., and Lee T. 1996. Toward an astrophysical theory of chondrites. *Science* 271:1545–1552.

Simon S. B., Davis A. M., Grossman L., and McKeegan K. D. 2002. A hibonite-corundum inclusion from Murchison: A first-generation condensate from the solar nebula. *Meteoritics & Planetary Science* 37:533–548.

Wasson J. T. and Kallemeyn G. W. 1990. Allan Hills 85085—A subchondritic meteorite of mixed nebular and regolithic heritage. *Earth and Planetary Science Letters* 101:148–161.

Weber D. and Bischoff A. 1994. The occurrence of grossite ($CaAl_4O_7$) in chondrites. *Geochimica et Cosmochimica Acta* 18: 3855–3877.

Weber D. and Bischoff A. 1997. Refractory inclusions in the CR chondrite Acfer 059—El Djouf 001: Petrology, chemical composition, and relationship to inclusion populations in other types of carbonaceous chondrites. *Chemie der Erde* 57:1–24.

Weber D., Zinner E., and Bischoff A. 1995a. Trace element abundances and magnesium, calcium, and titanium isotopic compositions of grossite-containing inclusions from the carbonaceous chondrite Acfer 182. *Geochimica et Cosmochimica Acta* 59:803–823.

Weber D., Schirmeyer S., and Bischoff A. 1995b. Refractory inclusions from the CH-chondrite PCA 91467: Similarities with and relationship to inclusions from ALH 85085 and Acfer 182 (abstract). 26th Lunar and Planetary Science Conference. pp. 1475–1476.

Weisberg M. K., Prinz M., and Nehru C. E. 1988. Petrology of ALH 85085: A chondrite with unique characteristics. *Earth and Planetary Science Letters* 91:19–32.

Weisberg M. K., Prinz M., Clayton R. N., Mayeda T. K., Sugiura N., Zashu S., and Ebihara M. 2001. A new metal-rich chondrite grouplet. *Meteoritics & Planetary Science* 36:401–418.

Yoshitake M. and Yurimoto H. 2004. Oxygen isotopic distributions among chondrules in Acfer 214, CH chondrite (abstract). Workshop on Chondrites and the Protoplanetary Disk. pp. 229–230.